Propagation of short fatigue cracks

S. Suresh and R. O. Ritchie

Fatigue crack propagation in engineering materials has been the subject of considerable research, and extensive review articles have appeared over the past several years. Most of these investigations focused on the behaviour of 'long' fatigue cracks, even though the characteristics associated with the extension of small cracks in metals and alloys remain relatively unexplored, despite their unquestionable importance from an engineering standpoint. In this review, the mechanics and micromechanisms of the subcritical growth of short fatigue cracks are examined, and aspects of their propagation behaviour are contrasted with those of long cracks in terms of fracture mechanics, microstructure, and environment. Cracks are defined as being short (i) when their length is small compared to relevant microstructural dimensions (a continuum mechanics limitation), (ii) when their length is small compared to the scale of local plasticity (a linear elastic fracture mechanics limitation), or (iii) when they are simply physically small (e.g. ≤ 0.5–1 mm). Since all three types of short flaw are known to propagate faster than (or at least at the same rate as) corresponding long fatigue cracks subjected to the same *nominal* driving force, current defect tolerant fatigue design procedures which utilize long crack data can, in certain applications, result in overestimates of lifetimes. The characteristics of the short crack problem are critically reviewed in the light of the influences of local plasticity, microstructure, crack tip environment, growth mechanisms, crack driving force, and the premature closure of the crack. IMR/137

Professor S. Suresh, BTech, MS, ScD, is in the Division of Engineering, Brown University, Providence, RI, USA. Professor R. O. Ritchie, MA, PhD, FIM, CEng, is in the Department of Materials Science and Mineral Engineering and the Lawrence Berkeley Laboratory, University of California at Berkeley, Cal., USA. Professor Suresh was formerly with the University of California at Berkeley.

LIST OF SYMBOLS

a = crack length

a_0 = intrinsic crack length, i.e. constant characteristic of material or material condition in expression for ΔK (equation (24))

Δa = increment of crack extension

da/dN = fatigue crack propagation rate

A = constant in cyclic constitutive law (Fig. 5)

b = sum of crack length a and blocked slip band zone w_0 (equations (18) and (19))

B = thickness of testpiece (Fig. 11)

c = depth of edge notch or half length of internal notch

$\bar{c}$ = half width of surface microcrack

C = experimentally determined scaling constant (equation (2))

d = proportionality factor dependent on yield strain ϵ_0 and work hardening exponent n (equation (13))

d_g = grain size

d_0 = maximum thickness of excess oxide layer

e = nominal difference in crack length between fatigue crack of length a in unnotched specimen and equivalent fatigue crack of length l growing from notch

E = elastic (Young's) modulus

E' = effective value of Young's modulus under different loading conditions

f = function of stress intensity factor range ΔK and load ratio R (equation (15))

f_{ij} = dimensionless function of polar angle θ measured from crack plane (equation (3))

f'_{ij}, f''_{ij} = universal functions of both polar angle θ measured from crack plane and work hardening exponent n (equation (10))

G = strain-energy release rate

J = scalar amplitude of crack tip stress and strain field under non-linear elastic conditions

ΔJ = cyclic component of J

k_f = fatigue strength reduction factor

k_t = theoretical elastic stress concentration factor

k_ϵ, k_σ = strain and stress concentration factors

K_{cl} = closure stress intensity factor

K_c^m = critical value of microscopic stress intensity at tip of slip band

K_I = stress intensity factor in mode I loading

K_{Ic} = critical stress intensity at failure (plane strain fracture toughness)

K_{II}^m = mode II value of microscopic stress intensity at tip of slip band (Fig. 17)

K_l = limiting stress intensity for long crack emanating from notch

K_{max}, K_{min} = maximum and minimum stresss intensities during cycle

K_s = limiting stress intensity for short crack emanating from notch

K_{th} = threshold stress intensity factor

K_0 = long crack threshold stress intensity factor

K_1, K_2 = local mode I and mode II stress intensity factors for non-linear crack

ΔK = nominal stress intensity factor range ($K_{max} - K_{min}$)

ΔK_{eff} = effective stress intensity factor range ($K_{max} - K_{cl}$)

ΔK_{eq} = equivalent stress intensity range for short crack

ΔK_i = initial stress intensity range

ΔK_{th} = threshold stress intensity factor range

ΔK_ϵ = pseudo-elastic–plastic strain intensity range

ΔK_0 = long crack threshold stress intensity factor range

l = length of crack growing from notch

l_0 = transition size of crack growing from notch

m = exponent in Paris power law (equation (2))

m' = exponent in power law for elastic–plastic fatigue crack growth (equation (12))

n, n' = monotonic and cyclic work hardening exponents, respectively

N = number of cycles

N_i = number of cycles necessary to initiate macrocrack

N_p = number of cycles necessary to propagate macrocrack subcritically until failure

P_{cl} = closure load during fatigue cycle

P_{max}, P_{min} = maximum and minimum loads during fatigue cycle

q = fraction of elastic strain with values between 0.5 and 1 (equation (22))

Q = dimensionless function of geometry (equation (8))

r = radial distance from crack tip

r_{max}, r_Δ = maximum and cyclic sizes of plastic zone

r_y = size of plastic zone

r_Δ^F = cyclic size of plastic zone at fatigue limit

R = load or stress ratio (K_{min}/K_{max})

R_ϵ = ratio of minimum to maximum strain (Fig. 24)

s = half distance between location of thickest oxide layer and crack tip

S = compliance of microcrack in completely opened state

w_0 = length of blocked slip band zone

$\Delta W_e, \Delta W_p$ = elastic and plastic components of of strain-energy density range

x = ratio of mode II to mode I crack tip displacements

α = empirical constant in Peterson k_f (equation (32))

β = constant in equation (36)

γ = non-dimensional fracture surface roughness factor

δ, δ_t = crack tip opening displacement

$\delta_{max}, \Delta\delta$ = maximum and range of crack tip opening displacement

$\delta(\sigma_{max})$ = crack tip opening displacement at maximum stress

$\delta(0)$ = crack tip opening displacement at zero load

$\Delta\delta_t$ = crack tip opening displacement range

ϵ = local strain

ϵ_p = plastic strain

ϵ_0 = yield strain

$\Delta\epsilon$ = local strain range

$\Delta\epsilon_e, \Delta\epsilon_p$ = elastic and plastic strain ranges

θ = polar angle measured from crack plane

θ_0, θ_1 = angles associated with crack deflection (Fig. 31)

ν = Poisson ratio

ρ = notch root radius

σ = local stress

σ^∞ = nominal stress

$\sigma_{cl}, \sigma_{max}$ = closure and maximum stresses

σ_e = tensile stress corresponding to fatigue limit

σ^*_{fr} = normal frictional stress for dislocation motion

σ_{ij} = local crack tip stresses dependent on distance from crack tip and inclination to crack plane

σ_{th} = threshold stress for no crack growth

σ_0 = yield or flow stress

$\Delta\sigma$ = local stress range

$\Delta\sigma^{\infty}$ = nominal stress range

$\Delta\sigma_e$ = fatigue limit or endurance strength

$\Delta\sigma_{th}$ = threshold stress range for no crack growth

τ^*_{fr} = shear frictional stress for dislocation motion (Fig. 17)

Fatigue fractures account for the vast majority of in-service failures in most engineering structures and components, either as a result of pure mechanical loading or in conjunction with sliding and friction between surfaces (fretting fatigue), rolling contact between surfaces (rolling contact fatigue), aggressive environments (environmentally assisted or corrosion fatigue) or elevated temperatures (creep fatigue). Such progressive fracture of materials by incipient growth of flaws under cyclically varying stresses, termed fatigue, can be categorized into the following discrete yet related phenomena:

(i) initial cyclic damage in the form of cyclic hardening or softening
(ii) creation of initial microscopic flaws (microcrack initiation)
(iii) coalescence of these microcracks to form an initial 'fatal' flaw (microcrack growth)
(iv) subsequent macroscopic propagation of this flaw (macrocrack growth)
(v) final catastrophic failure or instability.

In engineering terms the first three stages, involving cyclic deformation and microcrack initiation and growth, are generally classified together as (macro-) crack initiation, implying the formation of an 'engineering sized' detectable crack (e.g. of the order of several grain diameters in length). Thus, in such terms, the total fatigue life N can be defined as the number of cycles necessary both to initiate a (macro-) crack, N_i, and to propagate it subcritically until final failure, N_p, i.e.

$$N = N_i + N_p \quad . \quad . \quad . \quad . \quad . \quad . \quad . \quad . \quad (1)$$

In fatigue design, where data from laboratory sized specimens are used to predict the lifetime of more complex components in service (*see* Fig. 1 after Ref. 1), this distinction between initiation and propagation lives can be critical. Conventional approaches to fatigue design involve the use of S–N curves (stress *v.* number of cycles), representing the *total* life resulting from a given stress (or strain) amplitude, suitably adjusted to take into account effects of mean stress (using, for example, Goodman diagrams); effective stress concentrations at notches (using fatigue strength reduction factors or local strain analysis); variable amplitude loading (using the Palmgren–Miner cumulative damage law

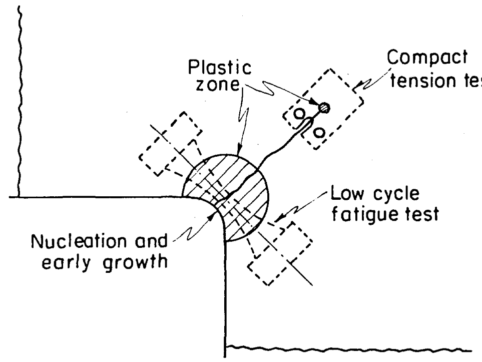

1 **Schematic diagram showing various stages of fatigue in engineering components and typical laboratory tests to evaluate fatigue life[1]**

or rainflow counting methods); multiaxial stresses; environmental effects; and so forth (for a summary, *see* Ref. 2). Although based on total life, this approach — which is in widespread use, particularly in the automotive industry — essentially represents design against crack *initiation*, since near the fatigue limit, especially in smooth specimens, most of the lifetime is spent in the formation of an engineering sized crack. In procedures for predicting lifetimes, such S–N or low cycle fatigue (LCF) testing might simulate the initiation and early growth of the fatigue crack within the fully plastic region of the strain field at some stress concentrator (*see* Fig. 1).

For safety-critical structures, especially those with welded and riveted components, the approach is different. There has been a growing awareness that the presence in a material of defects below a certain size must be assumed and taken into account at the design stage. Under such circumstances the integrity of a structure will depend on the lifetime spent in crack propagation, and since the crack initiation stage will be short, the use of conventional S–N total life analyses may lead to dangerous overestimates of life. Such considerations have led to the adoption of the so-called 'defect tolerant' approach in which the fatigue lifetime is assessed in terms of the time, or number of cycles, necessary to propagate the largest undetected crack to failure.[3] Here the initial size of the crack is estimated using non-destructive evaluation or proof tests, whereas the final size is defined in terms of the fracture toughness K_{Ic}, the limit load, or some allowable strain criterion. This approach, the only one used for certain applications in the nuclear and aerospace industries, for example, relies on the integration of an expression for crack growth, representing a fracture mechanics characterization of relevant fatigue crack propagation data suitably modified to account for mean stress effects (e.g. using the Forman equation), variable amplitude loading (e.g. using the Wheeler or the Willenborg model), environmental effects, and so forth, as required (for a summary, *see* Ref. 4). Such expressions are generally based on the original Paris power law relationship, i.e. are of the form

$$da/dN = C\Delta K^m \quad . \quad . \quad . \quad . \quad . \quad . \quad (2)$$

where C and m are experimentally determined scaling constants, da/dN is the crack growth increment per cycle, and ΔK is the alternating stress intensity factor given by the difference between the maximum and minimum stress intensities in the fatigue cycle ($\Delta K = K_{max} - K_{min}$).[5] In its simplest form equation (2) provides a reasonable description of growth rate in the so-called intermediate range of growth rates, typically between 10^{-6} and 10^{-3} mm/cycle. However, it underestimates propagation rates of higher values of ΔK, as final instability is approached (e.g. as $K_{max} \rightarrow K_{Ic}$), but overestimates propagation rates at lower values of ΔK approaching the so-called long crack fatigue threshold stress intensity range ΔK_0, below which long cracks remain dormant or grow at experimentally undetectable rates.[6] Since the time for crack initiation is generally taken to be zero, such defect-tolerant lifetime predictions are assumed to be inherently conservative and to simulate the macroscopic growth of the fatigue crack (*see* Fig. 1). In its most widely used form, that based on linear elastic fracture mechanics (LEFM), the latter approach would imply crack growth outside the notch strain field where the crack tip plastic zone is small compared to the crack length, i.e. that a long crack propagates under nominally elastic conditions.[5,6]

Current practice in the determination of the relevant crack growth 'law'* for a particular material under a particular set of conditions for a given application is to use data from laboratory tests on fatigue crack propagation, characterized in terms of the linear elastic stress intensity range ΔK. However, most of these data have been obtained from testpieces containing cracks of 25 mm or so, whereas many defects encountered in service are far smaller than this, particularly in turbine discs and blades, for example. In the relatively few cases where the fatigue behaviour of such short cracks has been studied experimentally (for earlier reviews, *see* Refs. 7–12), it has been found — almost without exception — that, under the same nominal driving force, the growth rates of short cracks are greater than (or at least equal to) the corresponding growth rates of long cracks (*see* Fig. 2). This implies a breakdown in the similitude concept generally assumed in fracture mechanics, as described in the section 'Similitude concept' below. Furthermore, it suggests that the use of data for long cracks in defect tolerant lifetime calculations for components where the growth of short flaws represents a large proportion of the lifetime, can lead to considerable overestimates.

There are several ways of defining 'short'† cracks:

(i) cracks which are of a length comparable to the scale of the microstructure (e.g. of the order of the grain size)

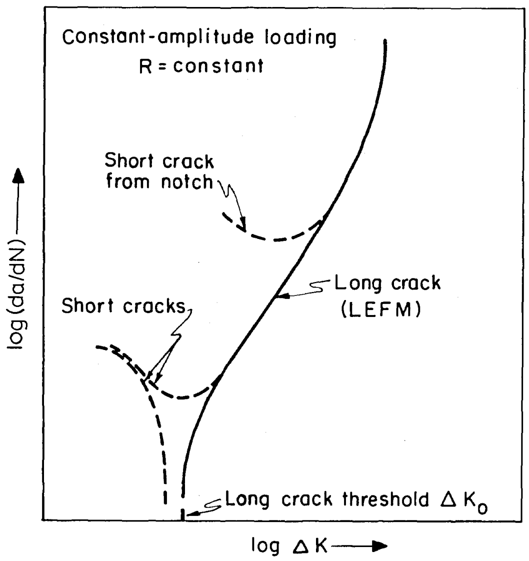

2 Typical fatigue crack propagation rates (da/dN) for long and short cracks as function of stress intensity factor range ΔK

(ii) cracks which are of a length comparable to the scale of local plasticity (e.g. small cracks embedded in the plastic zone of a notch or of a length comparable with their own crack tip plastic zones, typically $\leq 10^{-2}$ mm in ultrahigh strength materials and ≤ 0.1–1 mm in low strength materials)

(iii) cracks which are simply physically small (e.g. ≤ 0.5–1 mm).‡

Most investigations to date have focused on the first two factors, which represent, respectively, a continuum mechanics limitation and an LEFM limitation to current analyses. Here, presumably with an appropriate micro- or macro-mechanics characterization of crack advance, it should be possible to establish a correspondence between data for the growth rates of long and short cracks. However, physically short flaws, which are 'long' in terms of continuum mechanics and LEFM analyses, have also been shown to propagate more quickly than corresponding long cracks under the same nominal driving force (*see* e.g. Refs. 11 and 12). This may reflect basic differences in the physical micro-mechanisms associated with the extension of long and short cracks. Thus, physically short cracks represent a limitation in the similitude concept of fracture mechanics.

In this article is presented a review of the experimental results that have been obtained and of the ways in which the growth of short fatigue cracks in engineering materials has been interpreted. The literature on 'conventional' crack initiation and 'long' crack growth is examined only briefly since these are topics which have been given ample coverage in Refs. 4–7. However, a concerted effort has been made to review *all* the currently available information on short cracks. Since this is a rapidly expanding field some references may have inadvertantly been missed, and the authors regret any such omissions.

*Although often termed 'laws', such crack growth relationships are invariably totally empirical and are derived simply by fitting mathematical equations, of the form of equation (2), to sets of experimental data.

†A distinction is sometimes made between small cracks, which are small in all dimensions, and short cracks, which are small in all but one dimension (presumably the width), although such definitions are not considered in the present review.

‡Such physically small flaws are sometimes referred to as 'chemically small' where environmental effects are dominant.[11]

Situations in which short and long cracks may grow differently are discussed, from both an engineering and a mechanistic viewpoint, in terms of (i) appropriate fracture mechanics characterization and (ii) the physics and mechanisms involved in crack advance. In the former case the short crack problem is treated principally in terms of elastic–plastic fracture mechanics (EPFM) analyses in which the effects of local crack tip plasticity and the strain fields at notches are taken into account, whereas in the latter case differences in crack growth behaviour are examined in terms of the role of crack size and shape, microstructure, environment, and mechanisms for crack closure and extension. First, though, a brief summary is given of the fracture mechanics procedures used to characterize fatigue crack propagation for both long and short cracks.

FRACTURE MECHANICS CHARACTERIZATION OF FATIGUE CRACK GROWTH

Linear elastic fracture mechanics

The fracture mechanics approach to correlating cyclic crack advance begins with characterizing the local stress and deformation fields at the crack tip. This is achieved principally through asymptotic continuum mechanics analyses where the functional form of the local singular field is determined to within a scalar amplitude factor whose magnitude is calculated from a complete analysis of the applied loading and geometry. For the linear elastic behaviour of a nominally stationary crack subjected to tensile (mode I) opening, the local crack tip stresses σ_{ij} can be characterized in terms of the K_I singular field:[13,14]

$$\sigma_{ij}(r, \theta) = \frac{1}{(2\pi r)^{1/2}} K_I f_{ij}(\theta) + O(r^{1/2}) + \ldots$$

$$\lim_{r\to 0} \sigma_{ij}(r, \theta) = \frac{1}{(2\pi r)^{1/2}} K_I f_{ij}(\theta) \quad . \quad . \quad (3)$$

where K_I is the mode I stress intensity factor, r the distance ahead of the tip, θ the polar angle measured from the crack plane, and f_{ij} a dimensionless function of θ. Similar expressions exist for cracks subjected to pure shear (mode II) and anti-plane strain (mode III). Provided this asymptotic field can be considered to 'dominate' the vicinity of the crack tip, over a region which is large compared to the scale of microstructural deformation and fracture events involved, the scalar amplitude factor K_I can be considered as a single, configuration independent parameter which uniquely and autonomously characterizes the local stress field ahead of a linear elastic crack and can be used as a correlator of crack extension.

For cracks subjected to cyclically varying loads, K_I must be defined at the extremes of the cycle, such that a maximum and a minimum stress intensity (K_{max} and K_{min}, respectively) for a particular crack length can be computed. According to the original analysis by Paris and Erdogan,[15] the crack growth increment per cycle in fatigue, da/dN, can be described in terms of a power law function (equation (2)) of the range of K_I, given by the stress intensity range ΔK. It is important to note here that such an asymptotic continuum mechanics characterization does not require a detailed quantitative knowledge of the microscopic behaviour of individual fracture events, and thus the analysis is independent of the specific micromechanism of crack advance.

One of the principal limitations of this approach, specifically of the adoption of K_I as a valid description of the crack tip field, is that a state of small scale yielding must exist. From equation (3) it is apparent that as $r \to 0$, stresses become infinite at the tip. However, in reality such stresses are limited by local crack tip yielding, which occurs over a region ahead of the crack tip known as the plastic zone. Calculations of the extent of this region vary according to the mode of applied loading and the geometry of the body,[16] but a rough estimate of the size r_y of the plastic zone ahead of a monotonically loaded crack is given by

$$r_y \approx \frac{1}{2\pi}\left(\frac{K_I}{\sigma_0}\right)^2 \quad . \quad . \quad . \quad . \quad . \quad . \quad . \quad (4)$$

where σ_0 is the yield strength of the material. Provided this extent of local plasticity is small compared to the extent of the K_I-field, which is itself small compared to the overall dimensions of the body (including the crack length), the plastic zone can be considered as merely a small perturbation in the linear elastic field, and the K_I-field can be assumed to dominate the region around the crack tip. This situation, known as small scale yielding, occurs only when the size of the plastic zone is at most one-fifteenth of the in-plane dimensions of the crack length and the depth of remaining ligament.

The local yielding ahead of fatigue cracks is made somewhat more complex by reversed plasticity. However, following the analysis by Rice[17] of a cyclically stressed, elastic–perfectly plastic solid, plastic superposition of loading and unloading stress distributions can be used to compute the extent of the plastic zone ahead of a fatigue crack. On loading to K_{max}, a monotonic or maximum plastic zone is formed at the crack tip of dimension (from equation (4))

$$r_{max} \approx \frac{1}{2\pi}\left(\frac{K_{max}}{\sigma_0}\right)^2 \quad . \quad . \quad . \quad . \quad (5)$$

However, on unloading from K_{max} to K_{min}, superposing an elastic unloading distribution of maximum extent $-2\sigma_0$ gives rise to residual compressive stresses of magnitude $-\sigma_0$ in a region ahead of the crack tip. This region is known as the cyclic plastic zone, and its size r_Δ is approximately a quarter of the size of the monotonic zone:

$$r_\Delta \approx \frac{1}{2\pi}\left(\frac{\Delta K}{2\sigma_0}\right)^2 \quad . \quad . \quad . \quad . \quad . \quad . \quad . \quad (6)$$

where, strictly speaking, σ_0 is now the cyclic yield strength. Once again, the correlation of K_I with crack extension by fatigue will be a valid approach provided small scale yielding conditions apply, namely that r_{max} be small compared to the in-plane dimensions.

The numerical values of the stress intensity factors at the crack tip, K_I, ΔK, and so on, cannot be determined from the asymptotic analyses, yet can be computed from the overall geometry and applied loading conditions; in fact, solutions for K_I applicable to a wide range of conditions are now tabulated in handbooks.[18–20] A useful example of such K_I solutions which is particularly relevant to the short crack problem is that of a crack (of length l) growing from a notch (of length $2c$) – *see* Fig. 3. Modelling the notch as a circular hole in an infinite plate under a remotely applied tensile stress σ^∞, the limiting analytical K_I solution for a short crack emanating from the notch is obtained as

$$K_S = 1.12k_t\sigma^\infty(\pi l)^{1/2} \quad . \quad . \quad . \quad . \quad . \quad . \quad (7)$$

where k_t is the theoretical elastic stress concentration factor (equal to 3 here) and 1.12 is the free surface correction factor. However, when the crack becomes long the limiting stress intensity is obtained by idealizing the geometry so that the notch becomes part of a long crack of length $a = c + l$, such that

$$K_I = Q\sigma^\infty(\pi a)^{1/2} \quad . \quad . \quad . \quad . \quad . \quad . \quad (8)$$

where Q is a dimensionless function of geometry, such as a correction factor to allow for finite width. The numerically determined K_I solution for any crack emanating from a notch, shown by the dashed line in Fig. 3, can be seen to be given by the limiting cases of short and long cracks. As shown by Dowling,[21] the transitional crack size l_0, which can be interpreted as the extent of the local notch field, can then be obtained by combining equations (7) and (8) to give

$$l_0 = c/[(1.12k_t/Q)^2 + 1] \quad . \quad . \quad . \quad (9)$$

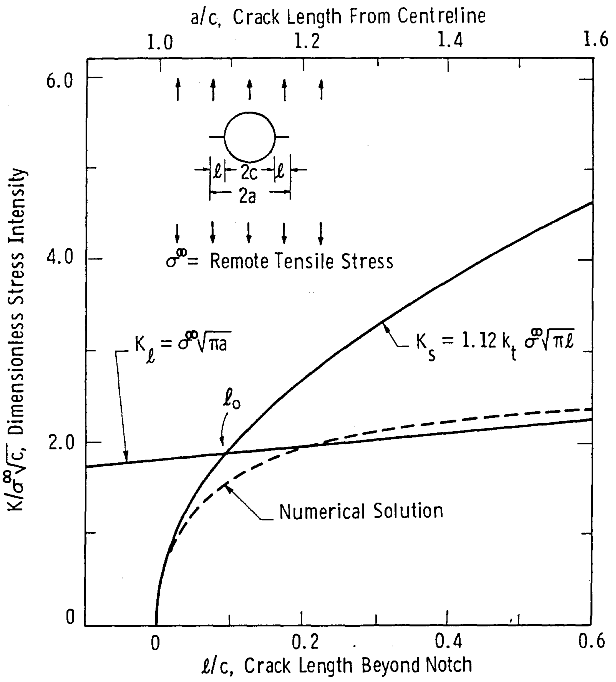

3 Linear elastic K_I solutions for crack of length l emanating from circular notch of radius c in an infinite plate subjected to remotely applied uniaxial tensile stress σ^∞; short crack (K_S) and long crack (K_I) limiting solutions and numerical solutions are shown[21]

Values of l_0 are generally a small fraction of the notch root radius ρ, and for moderate to sharp notches they generally fall in the range $\rho/20$ to $\rho/4$. Dowling[21] has further noted that $k_t\sigma^\infty$ values only 20–30% above σ_0 are sufficient to generate a notch tip plastic zone which engulfs the small crack region l_0 and thus, for small cracks at notches, LEFM analysis will often be suspect.

Elastic–plastic fracture mechanics

The above example serves to illustrate one aspect of the short crack problem, where the crack length is comparable with the size of the plastic zone around the notch tip. A similar situation, where small scale yielding conditions may not apply, is when the plastic zone at the tip of the fatigue crack itself is comparable with the crack length, i.e. when $a \sim r_y$. Since the use of K_I singular fields is no longer appropriate in such instances, alternative asymptotic analyses have been developed to define the crack tip stress and strain fields in the presence of more extensive local plasticity (for a recent review, *see* Ref. 22). Based on the deformation theory of plasticity (i.e. non-linear elasticity), the asymptotic form of these local fields for non-linear elastic power hardening solids obeying the constitutive law $\sigma \propto \epsilon_p^n$, is given by the Hutchinson–Rice–Rosengren (HRR) singularity as[23,24]

$$\left.\begin{aligned} \lim_{r\to o} \sigma_{ij}(r,\theta) &= (E'J/\sigma_0^2 r)^{n/(n+1)}\,\sigma_0 f'_{ij}(\theta,n) \\ \lim_{r\to o} \epsilon_{ij}(r,\theta) &= (E'J/\sigma_0^2 r)^{1/(n+1)}\, f''_{ij}(\theta,n) \end{aligned}\right\} \quad (10)$$

where n is the work hardening exponent, E' the appropriate elastic modulus ($= E$ for plane stress or $E/(1 - \nu^2)$ for plane strain), and f'_{ij} and f''_{ij} are universal functions of their arguments for plane stress and plane strain, respectively. The amplitude of this field is the so-called J-integral[25] and, analogous to K_I, J uniquely and autonomously characterizes the crack tip field under elastic–plastic conditions, provided there is some degree of strain hardening. Furthermore, for small scale yielding J can be directly related to the strain energy release rate G, and hence to K_I, i.e.

$$J = G = K_I^2/E' \qquad \text{(linear elastic)} \qquad (11)$$

Despite difficulties in establishing the precise meaning of J as applied to a description of the growth of cyclically stressed (non-stationary) cracks, Dowling[26] and Dowling and Begley[27] proposed a power law correlation of fatigue crack growth rates under elastic–plastic conditions to the range of J, i.e.

$$da/dN \propto \Delta J^{m'} \quad . \quad . \quad . \quad . \quad . \quad . \quad . \quad (12)$$

Provided such analysis is fundamentally justified, the use of ΔJ does present a first approach to characterizing the growth of short cracks which are comparable in size to the extent of local yielding. However, as mentioned above, the validity of the ΔJ approach is often questioned since it appears to contradict a basic assumption in the definition of J – that stress is proportional to the current plastic strain.[25] This follows because J is defined from the deformation theory of plasticity, which does not allow for the elastic unloading and non-proportional loading effects which accompany crack advance.[28] However, by recognizing that constitutive laws for cyclic plasticity (i.e. the cyclic stress–strain curve) can be considered in terms of stable hysteresis loops, and that such loops can be mathematically shifted to a common origin after each reversal, the criterion of stress being proportional to current plastic strain can effectively be satisfied for cyclic loading.[22,29]

An alternative treatment of elastic–plastic fatigue crack growth, which is not subject to the restrictions required by non-linear elasticity, is to use the concept of crack tip opening displacement (CTOD). From equation (10) it is apparent that the opening of the crack faces as $r \to 0$ varies as $r^{n/(n+1)}$ such that this separation can be used to define the CTOD (δ_t) as the opening where 45° lines emanating back from the crack tip intercept the crack faces. Thus, for proportional loading

$$\left.\begin{aligned} \delta_t &= d(\epsilon_0, n)\, J/\sigma_0^2 \quad &\text{(elastic–plastic)} \\ \delta_t &\propto K_I^2/\sigma_0 E' \quad &\text{(linear elastic)} \end{aligned}\right\} \qquad (13)$$

where d is a proportionality factor having a value of ~ 0.3–1 depending on the yield strain ϵ_0, the work-hardening exponent n, and whether plane stress or plane strain is assumed.[30] Since δ_t, like J, can be taken as a measure of the intensity of the elastic–plastic crack tip fields, it is feasible to correlate rates of fatigue crack growth to the range of δ_t, i.e. the cyclic CTOD $\Delta\delta_t$:

$$\left.\begin{aligned} da/dN &\propto \Delta\delta_t \quad &\text{(elastic–plastic)} \\ da/dN &\propto \Delta K_I^2/2\sigma_0 E' \quad &\text{(linear elastic)} \end{aligned}\right\} \qquad (14)$$

Approaches based on J and δ_t are basically equivalent for proportional loading, and are of course valid under both elastic–plastic and linear elastic conditions. Therefore, they are generally applicable to a continuum description of the growth rate behaviour of cracks that are considered small because their size is comparable with the scale of local plasticity. For such short cracks the use of EPFM rather than LEFM may thus be expected, at least in part, to normalize differences in behaviour between long and short cracks. However, the short crack problem is not simply a breakdown in the application of LEFM since the use of elastic–plastic analyses cannot totally normalize differences between short and long cracks. Although elastic–plastic analysis is certainly important, differences in the behaviour of long and short cracks can also be attributed to microstructural, environmental, and closure effects. Thus the short crack problem relates to a breakdown, not simply in LEFM, but in the fracture mechanics similitude concept.

Similitude concept

The application of fracture mechanics to the propagation of fatigue cracks is based on the premise that the governing parameter, such as the stress intensity factor K_I or the J-integral, used to correlate growth rates fully describes the stress and deformation fields in the vicinity of the crack tip. In addition, it is implicitly assumed that the concept of similitude (*see* Fig. 4) is valid. This concept implies that, for two cracks of different sizes subjected to the same stress intensity (under small scale yielding) in a given

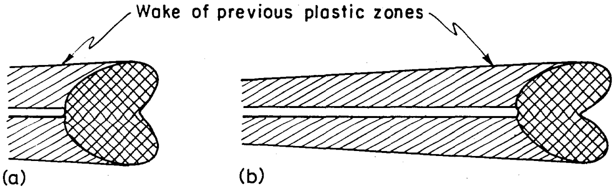

a short crack, $a \sim r_y$; *b* long crack, $a \gg r_y$

4 Schematic representation of similitude concept, which implies that cracks of differing length a subjected to same nominal driving force, e.g. ΔK, have equal plastic zone sizes r_y ahead of crack and will therefore advance by equal increments Δa per cycle

material–microstructure–environment system, crack tip plastic zones are equal in size and the stress and strain distributions along the borders of these zones (ahead of the crack) are identical. Accordingly, equal amounts of crack extension Δa are to be expected. For a cyclic load denoted by K_{max} and K_{min}, this dictates that

$$\Delta a = da/dN = f(K_{max}, K_{min}) = f(\Delta K, R) \qquad (15)$$

for each cycle, where the stress intensity range $\Delta K = K_{max} - K_{min}$ and the load ratio $R = K_{min}/K_{max}$. However, this concept of similitude cannot be applied when

(i) crack sizes approach the local microstructural dimensions
(ii) crack sizes are comparable with the extent of local plasticity for non-stationary flaws
(iii) through thickness, out of plane stresses (which are independent of K_I) are different
(iv) crack extension mechanisms are different
(v) extensive fatigue crack closure is observed
(vi) external environments significantly influence crack growth,

to name but a few instances.[10,12,31,32] Most of these mechanisms are specific to the short crack problem and thus contribute to differences in the growth rate behaviour of long and short cracks at nominally identical driving forces. They are discussed below in terms of local plasticity, and microstructural and environmental factors. In general, however, their effect on the breakdown of the similitude concept for short cracks is that they influence (to varying degrees according to the crack length, for example) the local driving force (i.e. the characterizing parameter K_I or J effectively experienced in the region near the tip). It is this 'near tip' parameter that governs crack advance, not the 'nominal' global value of this parameter computed by conventional analyses of externally applied loads and measurements of macroscopic crack lengths. In only a few instances have the relationships between the 'near tip' and the 'nominal' driving forces been quantified, indicating that the methodology for a global fracture mechanics analysis of short crack growth has yet to be developed.

EXPERIMENTAL TECHNIQUES

In the experimental measurement of the propagation and threshold behaviour of small fatigue cracks, many complex problems associated with reproducibility and scatter can be encountered. This is particularly true since most of the approaches used so far have involved adapting procedures originally designed for measuring long cracks.

Several experimental techniques are available for monitoring the growth rates of long fatigue cracks (*see* e.g. Refs. 33–35), including

(i) optical techniques (i.e. with the naked eye or travelling microscopes, or using high speed cameras)
(ii) methods based on measuring electrical resistance or potential using either dc or ac currents
(iii) compliance techniques using mouth opening (clip) or back-face strain gauges
(iv) acoustic emission
(v) ultrasonics
(vi) eddy current methods,

the first three being the most widely used. For long cracks, growth rates above 10^{-6} mm/cycle are generally measured by utilizing using such techniques at constant cyclic load levels (i.e. increasing ΔK with increasing crack length).[34] At levels near the threshold, on the other hand, crack growth rates ($da/dN \lesssim 10^{-6}$ mm/cycle) and threshold ΔK_0 values for long cracks are normally measured using the so-called 'load shedding' (decreasing ΔK) method (*see* e.g. Ref. 6). This procedure involves making continual reductions in ΔK (starting from an intermediate value) of not more than 10%. At each ΔK level, the crack is then allowed to propagate over a distance at least four times the size of the maximum plastic zone generated at the previous higher ΔK level. This load reduction scheme is repeated until the threshold ΔK_0 for no detectable (long) crack advance is reached. Such procedures,[6] typically used to monitor the growth and arrest of long fatigue cracks, pose extreme difficulties when adopted for measuring short cracks. Firstly, one faces the problem of estimating the depth of a short crack, emanating from a surface, from its width. This requires an empirical calibration and/or an educated guess. Also, with load shedding procedures used near the threshold, the crack is continually growing and so may cease to be 'short' by the time the threshold is reached. Moreover, the initiation stage of a 'major' short crack may involve the linking up of several flaws (e.g. from cracked inclusions) at different locations. While low magnification optical techniques are not particularly suited to detecting the presence and monitoring the growth of short cracks during a fatigue test, other methods such as the potential, resistance, or compliance teachniques may not have the required resolution and reproducbility to enable the growth of (part through) short cracks of complex geometry to be characterized. In addition to the difficulties associated with the limitations of the crack monitoring device, the growth of a short crack can be a strong function of local microstructural characteristics and environment (*see* e.g. Refs. 7–12). This aspect of short crack advance can also lead to poor reproducibility.

Since load shedding procedures are often difficult to apply, there is always the question of whether short crack behaviour should be studied using an artificial or a natural crack. It is particularly difficult to create an artificial notch without damaging the material immediately ahead of it, yet this is essential since it is this region in which short crack growth must be studied. The areas around machined notches contain residual stresses, whereas notches or starter cracks introduced by electro-discharge machining have a locally melted zone at their tip. Subsequent annealing cannot be guaranteed to remove such damage without drastically changing the microstructure under test. As discussed below, there are procedures in which a long crack is grown and material in its wake is then machined off to leave a short crack. Reproducibility is a major problem here, as is crack shape, since any amount of non-uniformity or 'bowing' in the original long crack will introduce irregular short cracks. However, one very successful method for rapidly initiating short cracks without causing significant damage, but only for aluminium alloys, has been to embrittle the sample surface before fatigue using small drops of ink at well separated locations.[36] Although the precise mechanism (involving some environmentally influenced fatigue process) is unknown, short cracks have been found to initiate extremely rapidly.

Initiation and growth measurements of short cracks

Optical techniques

Crack monitoring techniques using visual methods have probably been the most widely used procedures to date. For example, using procedures first adopted by Barsom and McNicol[37] for studying crack initiation, Fine and co-workers[38,39] have used a metallurgical microscope with a long working distance for visual and photographic observations of crack initiation and microcrack growth in wide, single edge notch (SEN) samples of steels and aluminium alloys. The microscope was mounted on an x–y micrometer base for positioning and measuring crack length. A camera attachment was available for photographically recording the progressive changes in the surface of specimens subjected to cyclic loading.

Morris and co-workers[40–49] used tapered flexural and hourglass shaped fatigue samples to monitor microcracks in aluminium and titanium alloys. Cracks were initiated on the surface of the specimen using various techniques, including making starter notches and marking with felt-tip pens. Crack propagation rates were estimated by monitoring crack size at regular intervals by transferring the specimen to a scanning electron microscope (SEM). The specimens were loaded in the SEM to estimate the microcrack tip opening displacement at the maximum load. For example, an empirical calibration equation was obtained for 2219 T851 aluminium alloy from several measurements of surface microcracks to estimate their depth a from a knowledge of their width $2c$. The expression

$$a/2\bar{c} = 0.362 + 25.01(\delta(\sigma_{max})/2\bar{c} - 0.015) \quad \ldots \quad (16)$$

was obtained,[47] where $\delta(\sigma_{max})$ is the CTOD at the maximum stress, σ_{max}.

Optical techniques have also been used to study short cracks at elevated temperatures. For example, Sheldon *et al.*[50] designed a microscope with a long working distance to monitor *in situ* the growth of short and long cracks in nickel-base superalloys at temperatures as high as 650°C. Cracks were initiated at high stress intensities at ambient temperature, whereupon the load was successively reduced until the approximate room temperature long crack threshold values were reached. Once load shedding was complete, the specimen was machined and polished to a configuration such that a crack only 0.06–0.16 mm long was left in the test panel. The cross-section of the specimen was a parallelogram containing the crack at one acute corner. Sheldon *et al.* claimed that the taper allows the location of the crack front to be defined more accurately, and that the crack in the taper interacted with only a small amount of material along its front. This was considered to be representative of a naturally occurring small crack.

Replication techniques

One of the most widely used techniques for monitoring the initiation and growth of small flaws has been the replication method. For example, Dowling[51,52] used cellulose acetate surface replicas for measuring the growth of short cracks during low cycle fatigue tests on smooth axial specimens of A533B steel. Tests were interrupted periodically for replicating with ~0.1 mm tape, softened with acetone to gain an impression of the specimen surface. The propagation rates of such surface flaws (of length 0.25–1.75 mm) were characterized in terms of EPFM, specifically involving ΔJ. Procedures for calculating J from the loading portion of the fatigue cycle, summarized in Fig. 5, involve the following approximations:[51]

(i) surface cracks were assumed to have depth a equal to half their surface length $2c$

(ii) ranges of stress and plastic strain, obtained from stable cyclic hysteresis loops, were used to quantify ΔJ

(iii) the value of ΔJ for such semicircular surface crack geometries was given by:

$$\Delta J \simeq 3.2\Delta W_e a + 5.0\Delta W_p a \quad . \quad . \quad (17)$$

where ΔW_e and ΔW_p are the elastic and plastic components of the remote strain energy density ranges (*see* Fig. 5)

(iv) the scaling constants in equation (17), which incorporate correction factors for specimen geometry and flaw shape, were derived from equivalent linear elastic solutions.

In the general sense, there are problems with using either optical or replication techniques in that they are difficult to apply in hostile environments, such as in corrosive solutions or at elevated temperatures. More importantly, they give information only on the surface length of the crack, and therefore assumptions must be made if the internal profile is to be estimated.

Electrical potential techniques

Electrical potential techniques have also been developed for studying short cracks. Gangloff, for example, quantified the formation and subcritical propagation of small cracks emanating from artificial surface defects.[11,53,54] Flaws were introduced along a chord of an hourglass type (low cycle fatigue) specimen (at the minimum diameter) by either conventional grinding or electrospark discharge machining. The crack depth was continuously monitored via dc electrical potential measurements and an analytical calibration model,[53] and was found to agree reasonably well with the corresponding values measured optically. The calibration model used was claimed to account for crack shape as well as variations in depth for the elliptical surface flaws utilized in the experiments. This technique is particularly suitable

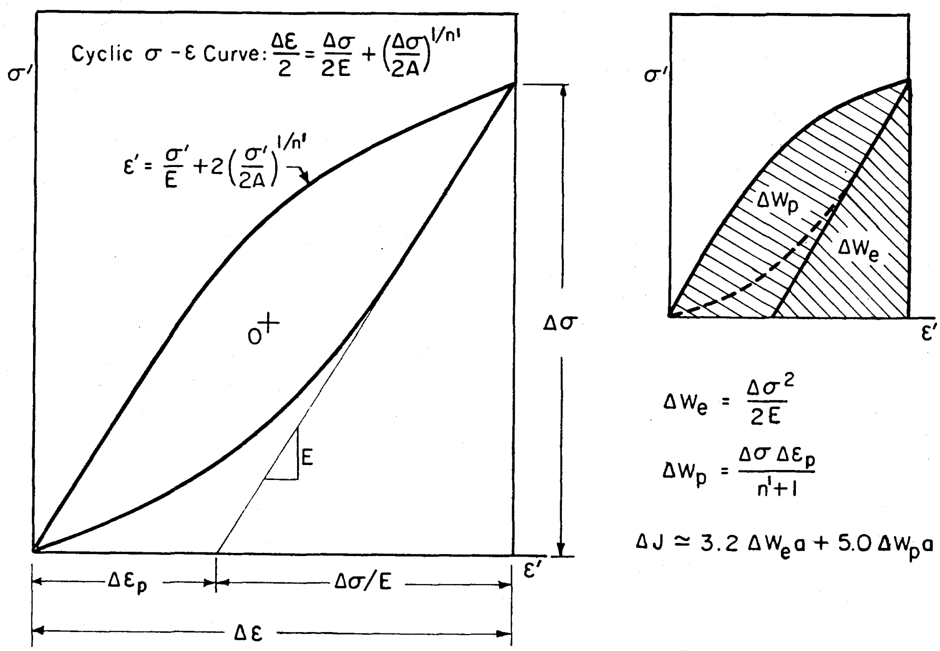

5 Procedure for estimating ΔJ from stress–strain hysteresis loops for growth of small cracks during low cycle fatigue of smooth axial specimens[51]

for physically short cracks, i.e. those 0.5–1 mm long, and so has been effective in gaining information on the growth of short fatigue cracks in higher strength materials. Furthermore, since it is a remote monitoring technique it can be applied even in aggressive environments.

Other techniques

Several other techniques have been proposed for the detection and monitoring of small flaws, and many, although still in the development stage, show excellent promise for obtaining measurements in the micrometre–millimetre range. For example, Nelson and co-workers[55] have utilized a method of monitoring surface acoustic waves to quantify the depth and crack closure characteristics of microscopic surface fatigue cracks. Using acoustic measurements of the reflection coefficient of Rayleigh waves incident on the crack, coupled with optical measurements of surface crack length, these authors were able to claim good accuracy over a range of crack aspect ratios for depths between 50 and 150 μm (Ref. 55). Several electrochemical methods have also been proposed for the early detection of microscopic fatigue damage, notably by Baxter.[56] Accuracies of ±10 μm have been reported for the detection of small fatigue cracks in both steels and aluminium alloys through the identification of locations where such cracks rupture the surface oxide film. Such rupture sites are imaged using photoelectron microscopy and, more recently, by measuring the re-anodization current or with the aid of a gel containing iodine.[56]

Measurements of short crack thresholds

The load shedding procedure commonly used to obtain the threshold ΔK_0 for no detectable propagation of long cracks is not readily applicable to short cracks (those of a size smaller than the local plastic zone or the characteristic microstructural dimension) because of the need to reduce the load to threshold levels over a considerable distance of crack growth. However, the procedure can be used for physically short (0.1–0.8 mm) cracks in ultrahigh strength materials where both the scale of local plasticity and the grain size are smaller than the crack depth, and load shedding procedures can be sufficiently rapid to enable the near-threshold region to be approached over small increments of crack advance (*see* e.g. Ref. 57).

Wiltshire and Knott[58] used two different methods to obtain short 'through-thickness' and 'thumbnail' cracks in a study of the effect of crack length on fracture toughness. Such procedures seem suitable for use in evaluating growth and thresholds for short cracks. For through-thickness cracks in maraging steels a long crack was first produced by fatiguing SEN specimens in bending, as shown in Fig. 6*a*, with the sample in the solution annealed condition. Short through-thickness cracks were then obtained by grinding away the upper surface, and the samples were subsequently aged to develop full strength. Similar procedures were used to produce short 'thumbnail' cracks, as shown in Fig. 6*b*. The two top edges of a bend specimen were machined away to leave a ridge along the centre, a slot was introduced in the ridge, and the specimen was fatigue precracked in bending. The

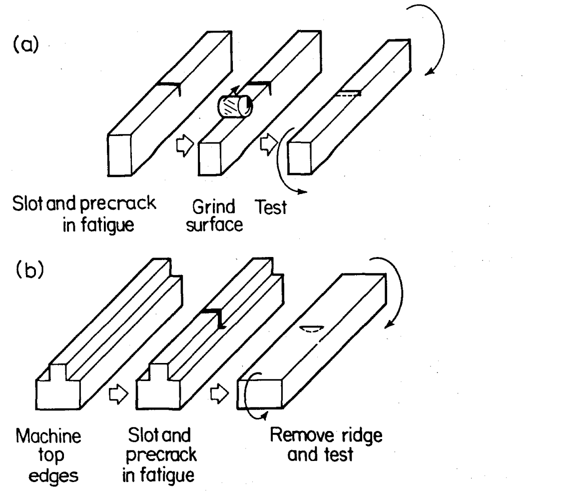

a through thickness crack; *b* thumbnail crack

6 Ways of preparing short cracks[58]

fatigue crack was found to propagate down the ridge as a straight fronted crack, and then into the bulk of the specimen with a semi-elliptical crack front. Its depth was controlled by stopping the bending after it had spread a certain distance across the prepolished shoulders. Finally, the ridge was removed to leave a semi-elliptical surface crack in the remaining rectangular section.

Such procedures have been used to produce through-thickness and part-through-thickness short cracks to measure the thresholds for the arrest of short cracks.[59–62] Usami and Shida,[59] for example, used this technique to measure fatigue thresholds in a range of steels for crack sizes between 0.1 and 0.3 mm. McCarver and Ritchie[60] used similar procedures to monitor the thresholds for physically short cracks in a wrought nickel-base superalloy, René 95. In both these investigations fatigue precracking was performed under a far-field cyclic compressive load on bend specimens. This results in growth and arrest of the precrack to a predictable depth which is a function of the size of the plastic zone as computed from the compressive loads. Such compression gives rise to residual tensile stresses which apparently act as the driving force for crack growth.* Following precracking and machining away of most of the crack, the samples were annealed in an attempt to minimize possible damage in the vicinity of the short crack tip. McCarver and Ritchie[60] subsequently measured short crack thresholds in such specimens, using a procedure analogous to defining a fatigue limit in unnotched specimens. Samples were cycled at different initial stress intensity ranges ΔK_i, and the short crack threshold defined in terms of the largest value of ΔK_i which did not cause failure (or any

*Recent studies by Suresh[63] on crack initiation under compression in a wide range of alloys have revealed that cracks arrest at a length approximately equal to the cyclic plastic zone size in compression. However, at high cyclic compressive loads it was found that crack arrest can occur at critical lengths independent of applied load, apparently as a result of the development of closure behind the crack tip.

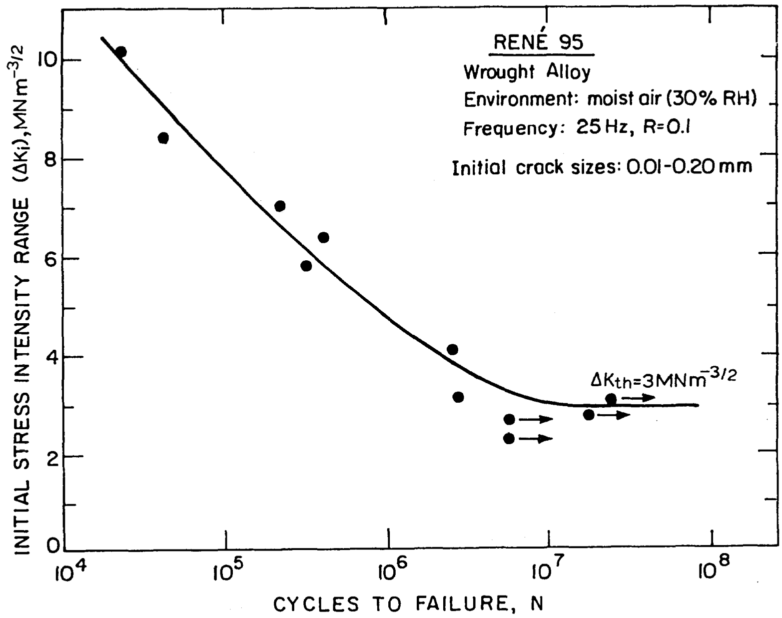

7 **Variation of initial stress intensity ΔK_i with number N of cycles to failure for physically short cracks in wrought René 95 ($\sigma_0 = 1400$ MNm^{-2}), showing definition of threshold ΔK_{th} for 0.01–0.2 mm cracks, fatigue tested in moist air at 25 Hz and $R = 0.1$ (Ref. 60)**

evidence of crack growth) in 10^8 cycles (*see* Fig. 7).

Measurement of closure of short cracks

The techniques available for routine monitoring of the premature closure of long fatigue cracks generally cannot be used for short cracks (whose growth involves considerable geometrical changes, and whose measurement suffers from irreproducibility and scatter) which demand far superior resolution in measurements. Closure in long fatigue cracks has been measured using optical techniques, compliance techniques, methods involving electrical resistance or potential, acoustic emission, and ultrasonics (*see* e.g. Refs. 33 and 34). Most of these techniques do not seem suitable for use with short cracks because of their insufficient resolution, insensitivity to short crack shape and geometry, and irreproducibility.

Early studies of crack closure for short cracks were carried out by Morris and Buck,[41] who used a compliance technique to determine the closure load for surface microcracks of up to one grain size produced in triangular specimens of aluminium alloys subjected to fully reversed loading. Scanning electron microscopy was then used to measure the compliance of surface microcracks. A 'home-made' fixture incorporated in the electron microscope was utilized to apply known loads to the samples *in situ*. High resolution micrographs of the crack were obtained at different load (stress) levels, from which the crack opening δ was estimated. Figure 8 shows a typical compliance curve for a microcrack obtained for 2219 T851 aluminium alloy. Morris and Buck defined the following parameters to characterize crack closure: $\delta(0)$, the crack opening displacement at zero load, σ_{cl}/σ_{max}, the closure stress ratio (taken to be the value of σ/σ_{max} at the inflection point in the stress–displacement curve), and $S = \Delta\delta/\Delta(\sigma/\sigma_{max})$ measured for $\sigma > \sigma_{cl}$, where S is a measure of the compliance of the microcrack in the completely opened state.

Compliance techniques were also used by Tanaka and Nakai[61,64] for measuring crack closure levels to examine the growth of short cracks emanating from notched centre-cracked specimens of a structural low carbon steel. Here, the hysteresis loop of load v. CTOD at the centre of the crack was recorded intermittently during the test, and the point of crack opening was determined as the inflection point of compliance,

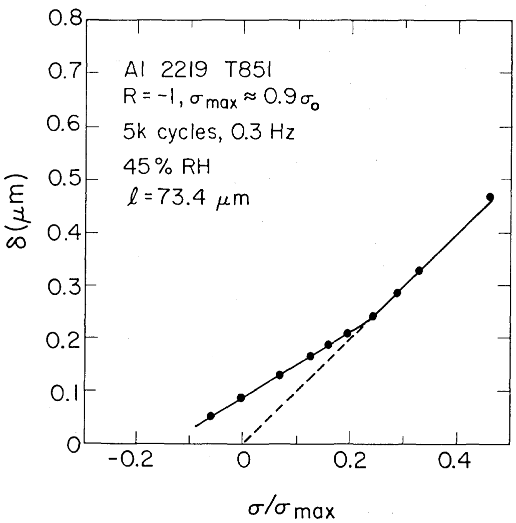

8 **Typical microcrack compliance curve for 2219 T851 aluminium alloy; δ is opening across microcrack, and σ/σ_{max} fraction of maximum load applied during fatigue[41]**

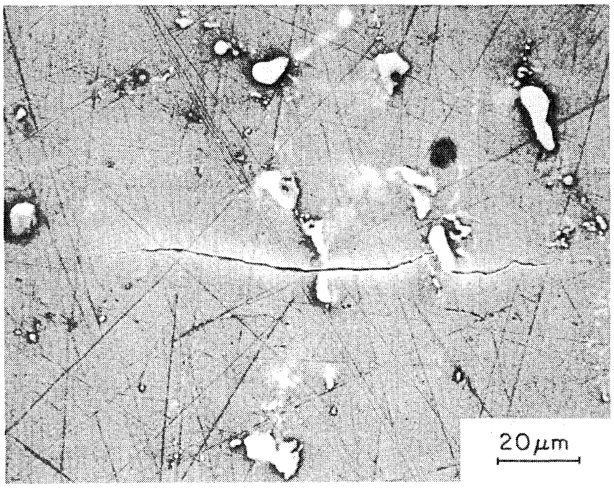

9 Appearance of typical surface microcrack initiated at β-phase (Cu_2FeAl_7) intermetallic in 2219 T851 aluminium alloy fatigue tested in humid air[45]

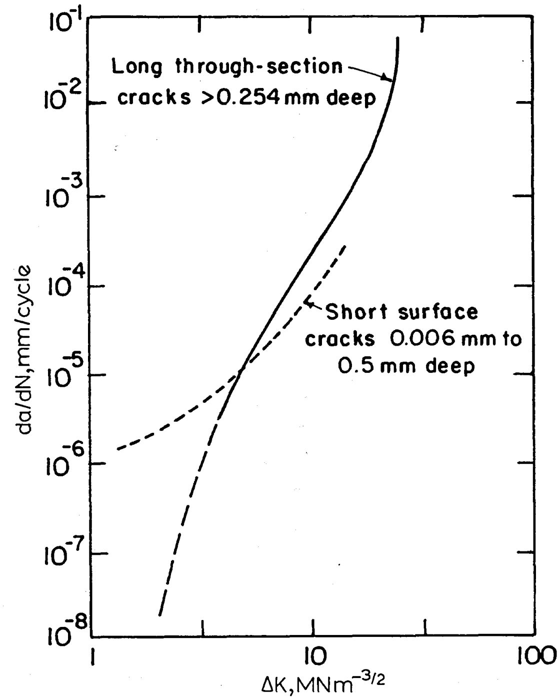

10 Difference in propagation rates d*a*/d*N* of fatigue cracks as function of stress intensity factor range Δ*K* for precipitation hardened aluminium alloys[68]

magnified by a circuit subtracting the elastic compliance from the loading curve.

Recently, procedures have been developed to monitor the behaviour of short fatigue cracks, using stereo-imaging techniques and *in situ* analyses in the SEM.[65,66] Such methods enable the crack opening (mode I) and sliding (mode II) displacements to be measured directly as functions of load for both short and long cracks subjected to cyclic loads within the electron microscope.

RESULTS ON GROWTH OF SHORT FATIGUE CRACKS

Microstructural effects

The first definition of a short fatigue crack (*see* the introductory section) refers to cracks which are of a size comparable to the scale of characteristic microstructural features. Figure 9 shows a micrograph of such a typical surface microcrack initiated at a β-phase (Cu_2FeAl_7) intermetallic in 2219 T851 aluminium alloy, taken from work by Morris.[45] A number of recent experimental studies[7–12,37–49,67–76] on the initiation and growth of cracks in a wide range of materials have revealed that such short cracks, initiated near regions of surface roughening caused by the to and fro motion of dislocations or at inclusions and grain boundaries, propagate at rates which are different from those of equivalent long cracks when characterized in terms of conventional fracture mechanics concepts. For example, it was first shown by Pearson[68] that in precipitation hardened aluminium alloys, cracks of a size comparable to the average grain diameter grew several times as quickly as long cracks at nominally identical alternating stress intensities (Fig. 10). Other studies of mild steels[69] (Fig. 11), silicon iron[70] (Fig. 12) and peak aged 7075 aluminium alloy[71] (Fig. 13), for example, clearly reveal this lack of correspondence between data for long and for microscopically short cracks. However, the results obtained by Lankford[71,72] and

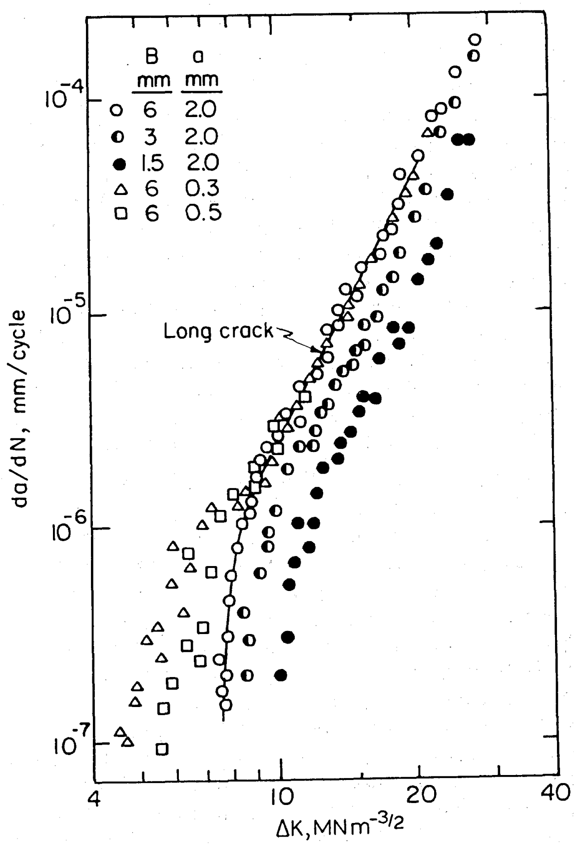

11 Difference in propagation rates d*a*/d*N* of short and long fatigue cracks as function of stress intensity factor range Δ*K* for 0.035%C mild steel of yield strength σ_0 = 242 MNm^{-2}

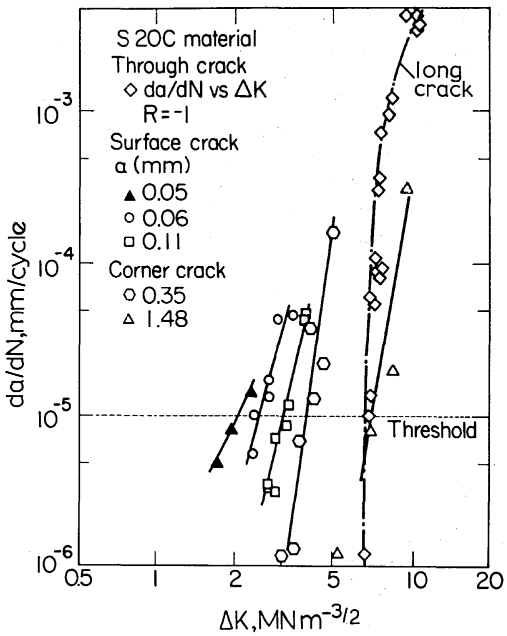

12 **Difference in propagation rates da/dN of short and long fatigue cracks as function of stress intensity factor range ΔK for 3%Si iron of yield strength σ_0 = 431 MNm^{-2} (Ref. 70)**

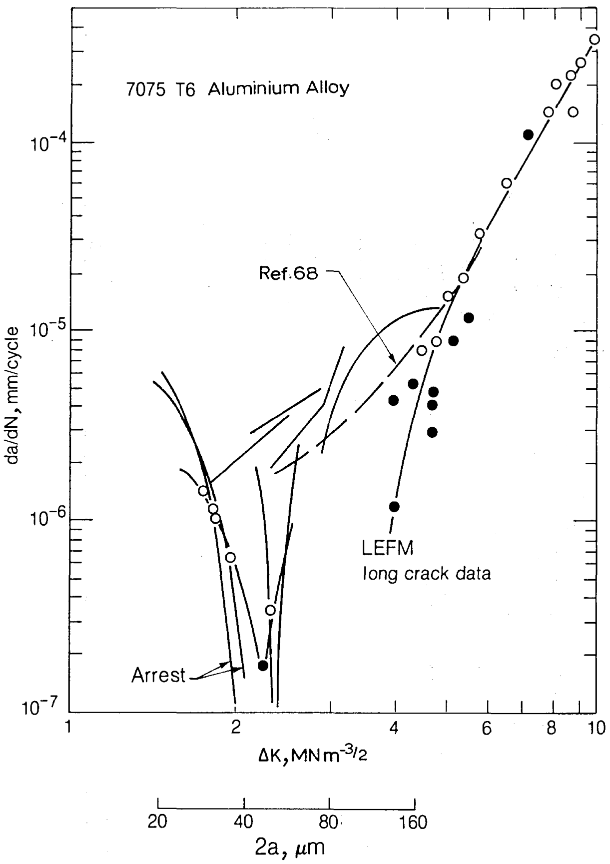

13 **Difference in propagation rates da/dN of short and long fatigue cracks as function of stress intensity factor range ΔK for peak aged Al–Zn–Mg alloy (7075 T6) of yield strength σ_0 = 515 MNm^{-2} (Ref. 71)**

others[39,49,69,70,73,74] have shown that there is generally a consistent trend to this variation between growth rates for long and short cracks. This trend is depicted clearly in Fig. 14 for 7075 T6 aluminium alloy, in which growth rates for long and for microscopically short (i.e. of a size comparable with the grain diameter) cracks are plotted as a function of the linear elastic stress intensity range.[71] It is apparent from this figure that the growth rates associated with the short cracks are up to two orders of magnitude faster than those of the long cracks, and further that such accelerated short crack advance occurs at stress intensity ranges well below the long crack fatigue threshold stress intensity range (ΔK_0).[71] The initially higher growth rates of the short cracks can be seen to decelerate progressively (and even arrest in certain cases) before merging with the long crack data at stress intensities close to ΔK_0, similar to observations reported elsewhere by Morris and co-workers,[42–46] Kung and Fine,[39] Tanaka and co-workers,[70,75,76] Taylor and Knott,[73] and others. The progressively decreasing growth rates of the short cracks below the long crack threshold is intriguing since in terms of conventional analyses one would imagine the nominal driving force for crack advance (e.g. ΔK) to increase with increasing crack length (e.g. as given by equations (7) and (8)), thereby leading to progressively increasing growth rates. However, the behaviour of microscopically short cracks has been rationalized in terms of a deceleration of growth as a result of crack closure and through interactions with microstructural features – particularly grain boundaries.[12,42–47,69–76] For example, specific observations of grain boundaries impeding the growth of short cracks have been reported for aluminium alloys,[42–46,71,72] nickel-base superalloys,[50] tempered martensitic high strength steels,[77,78] and lower strength mild steels.[75,76] Using arguments based on microplasticity and crack closure effects, Morris and

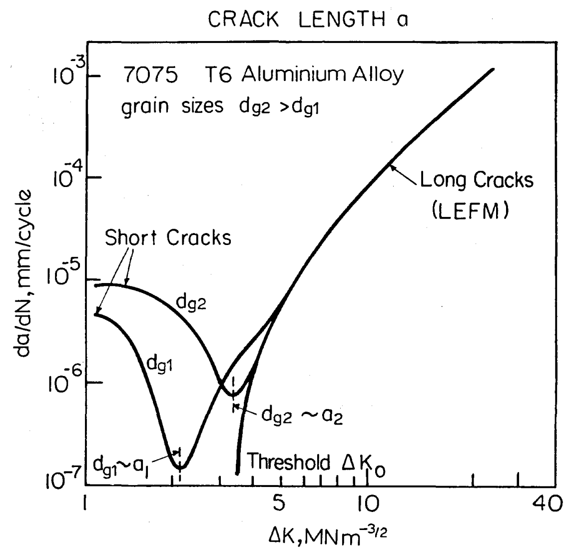

14 **Effect of grain size d_g on growth of microstructurally short and long cracks in 7075 T6 aluminium alloy σ_0 = 515 MNm^{-2}; microcracks grow below long crack threshold ΔK_0 and show growth rate minima approximately where crack length $a \sim d_g$ (Ref. 71)**

co-workers[44-49] have modelled the process in terms of two factors: the cessation of propagation into a neighbouring grain until a sizeable plastic zone is established, and a retardation in growth rates caused by an elevated crack closure stress. Tanaka and co-workers[76,79,80] similarly considered the impeded growth of microstructurally short cracks in terms of the pinning of slip bands, emanating from the crack tip, by the next grain boundary. The results obtained by Lankford[71] and shown in Fig. 14 indicate that the minimum crack growth rate appears to correspond to a crack length roughly equal to the smallest grain dimension (i.e. $a \sim d_g$). Furthermore, the depth of the deceleration 'well' appears to be determined by the degree of microplasticity involved in the crack traversing the boundary. For example, when the orientation between the grain containing the crack and the neighbouring grain was similar, there was little deceleration in growth rates at the boundary. Thus a consensus from these studies is that, despite their propagating faster than long cracks,

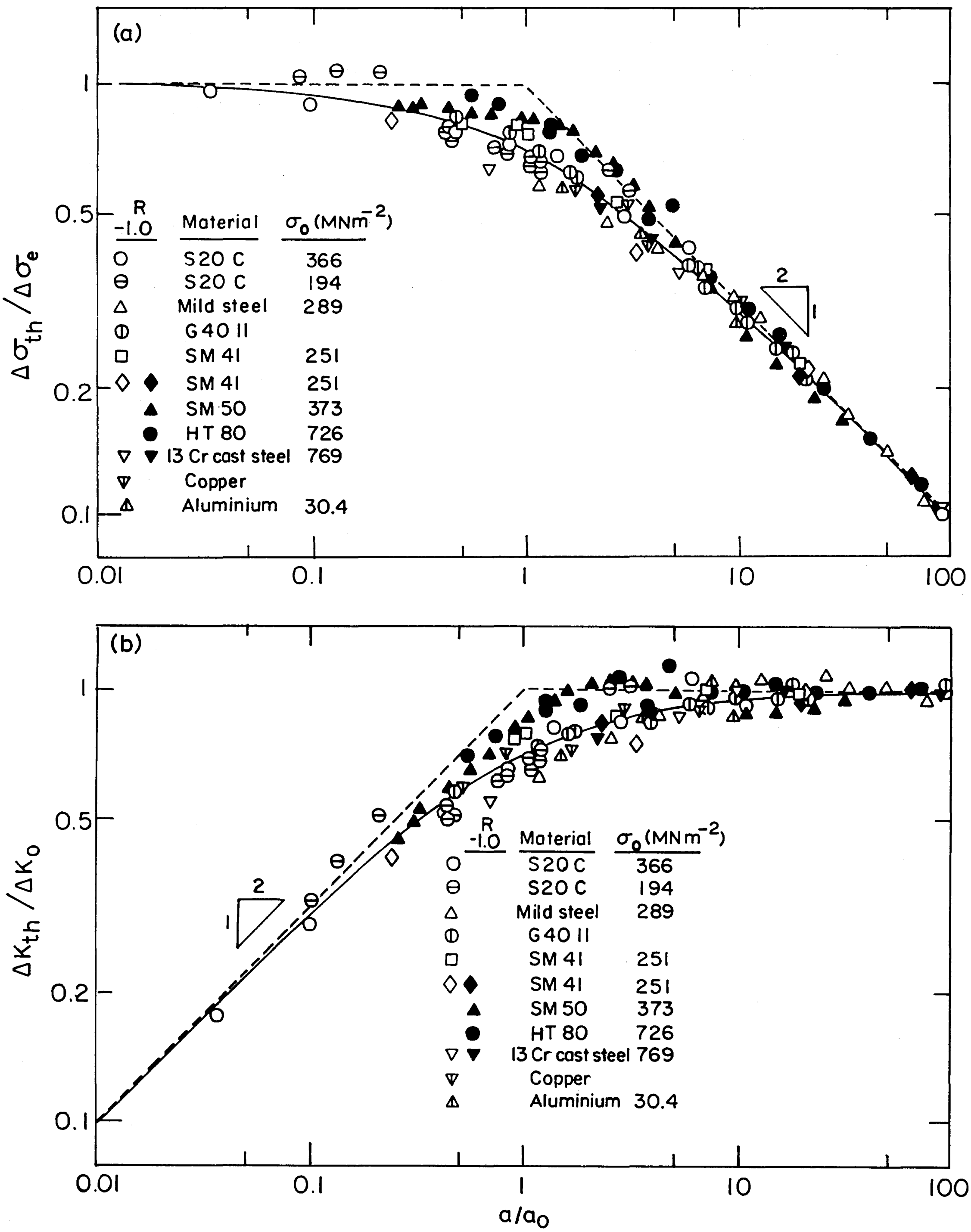

a threshold stress $\Delta\sigma_{th}$, normalized with respect to smooth bar fatigue limit $\Delta\sigma_e$; *b* threshold stress intensity range ΔK_{th}, normalized with respect to long crack threshold ΔK_0

15 Variation of threshold stress and stress intensity with crack length *a*, normalized with respect to intrinsic crack length $a_0 = (1/\pi)(\Delta K_0/\Delta\sigma_e)^2$ (Ref. 76)

short cracks are apparently impeded by the presence of grain boundaries, which in general would be unlikely to affect significantly the local propagation rates of long cracks. The extent of reductions in the effective driving force for various degrees of such short crack deflections at grain boundaries has recently been calculated by Suresh.[81] It is the present authors' opinion that the interaction of short cracks with microstructural features, which leads to the apparent progressive deceleration of short cracks below the value of ΔK_0 for long cracks, results principally from crack deflection[81] and associated crack closure[12,61] mechanisms. The specific evidence for this is examined in the 'Discussion' section below.

From such experimental studies, it is readily apparent that threshold stresses (or stress intensities) associated with long and short cracks are likely to be very different. Conventional fracture mechanics arguments imply that the threshold stress intensity range (ΔK_{th}) for a particular material should be independent of crack length (i.e. $\Delta K_{th} = \Delta K_0$, the long crack threshold, is constant). Kitagawa and Takahashi,[82] however, first showed that below a critical crack size the threshold ΔK_{th} for short cracks actually decreased with decreasing crack length, where the threshold stress $\Delta\sigma_{th}$ approached that of the smooth bar fatigue limit $\Delta\sigma_e$ at very short crack lengths (*see* e.g. Fig. 15). Typical experimental data showing this decay in the threshold stress intensity range ΔK_{th} at short crack lengths are shown in Fig. 16, taken from the results obtained by Romaniv *et al.*[69] for annealed mild steel, 0.45%C austenitic steel, and an Al–Zn–Mg alloy. Several workers have

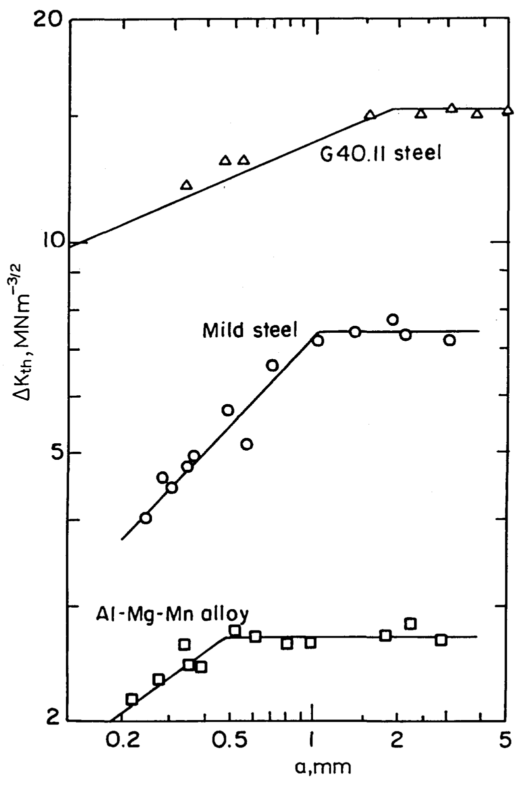

16 Variation of threshold stress intensity range ΔK_{th} with short crack length a in G40.11 austenitic 0.45%C steel, $\sigma_0 = 550$ MNm^{-2}, 0.035%C mild steel, $\sigma_0 = 242$ MNm^{-2}, and Al–Zn–Mg alloy, $\sigma_0 = 180$ MNm^{-2} (Ref. 69)

claimed that the critical crack size (below which ΔK_{th} is no longer constant with crack size) depends on microstructural and mechanical factors.[8–10,12,47,64,69–76,80–83] It has even been suggested, for example, that this critical crack length above which LEFM is applicable is simply ten times the characteristic microstructural dimension.[83] However, from continuum mechanics arguments, an estimate of this crack size can be obtained in terms of $(1/\pi)(\Delta K_0/\Delta\sigma_e)^2$, with both ΔK_0 and $\Delta\sigma_e$ corrected for a common load ratio. Typical values of this dimension, which effectively represent the limiting crack size for valid LEFM analysis (*see* the section 'Fracture mechanics characterization of fatigue crack growth' above), vary from 1–10 μm in ultrahigh strength materials (i.e. $\sigma_0 \sim 2000$ MNm^{-2}) to 0.1–1 mm in low strength materials (i.e. $\sigma_0 \sim 200$ MNm^{-2}).[12]

From such experimental results it is generally concluded that the threshold condition for no growth for long cracks is one of a constant stress intensity, i.e. ΔK_0, whereas the threshold condition for short cracks is one of a constant stress, i.e. the fatigue limit $\Delta\sigma_e$ or the endurance strength. Such a premise has been shown to be consistent with the models derived by Tanaka *et al.*[76] in which the threshold for short crack propagation is governed by whether the crack tip slip bands are blocked, or can traverse the grain boundary to an adjacent grain. This condition governing whether the slip band is blocked, shown in Fig. 17 in terms of a critical value of the microscopic stress intensity K_c^m at the tip of the band, yields expressions for the fatigue threshold stress σ_{th} and stress intensity K_{th}:

$$\sigma_{th} = \frac{K_c^m}{(\pi b)^{1/2}} + \frac{2}{\pi}\,\sigma_{fr}^{\star}\cos^{-1}(a/b) \quad . \quad . \quad (18)$$

$$\begin{aligned} K_{th} &= \sigma_{th}\,(\pi a)^{1/2} \\ &= K_c^m (a/b)^{1/2} \\ &\quad + 2(a/\pi)^{1/2}\sigma_{fr}^{\star}\cos^{-1}(a/b) \quad . \quad . \quad (19) \end{aligned}$$

Here, for a slip band coplanar to the crack plane in the two dimensional model shown in Fig. 17, b is the crack length a plus the width w_0 of the blocked slip band zone, and $\sigma_{fr}^{\star}$ is the frictional

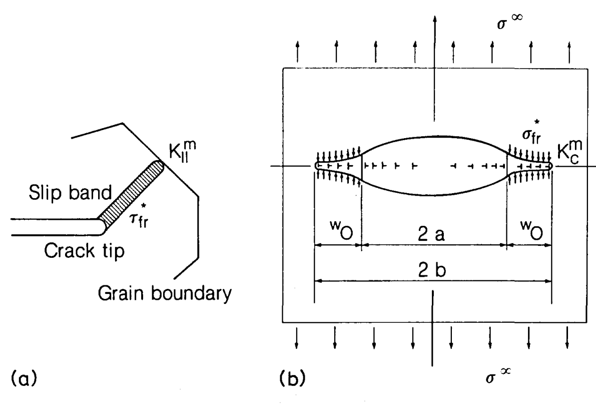

17 Schematic illustration of *a* crack tip slip band blocked by grain boundary and *b* coplanar slip band emanating from tip of isolated crack[76]

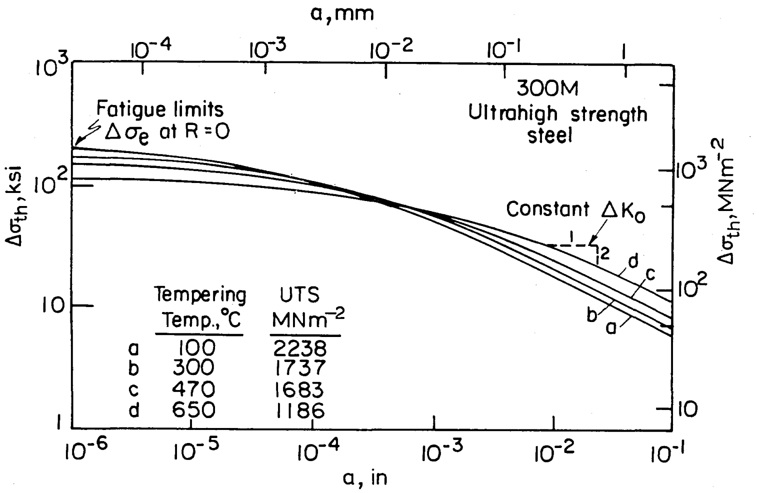

18 **Predicted variation of threshold stress $\Delta\sigma_{th}$ at $R = 0$ with crack length a based on data for 300M ultrahigh strength steel (silicon modified AISI 4340), oil quenched and tempered between 100 and 650°C to vary tensile strength (1186 to 2338 MNm^{-2}) (Ref. 6)**

stress for dislocation motion in the band. The long crack threshold stress intensity K_0 thus follows from equation (19) by taking the limit of K_{th} when $w_0 \ll a$, i.e.

$$K_0 = K_c^m + 2(2/\pi)^{1/2}\sigma_{fr}^\star w_0^{1/2} \quad . \quad . \quad . \quad (20)$$

whereas the short crack threshold stress, i.e. the fatigue limit σ_e, follows from equation (18) at $a = 0$, i.e.

$$\sigma_e = \sigma_{fr}^\star + K_c^m/(\pi w_0)^{1/2} \quad . \quad . \quad . \quad . \quad (21)$$

Since, at the fatigue limit, the slip band can be considered to be constrained within a single grain, w_0 can be assumed to be approximately half the grain size d_g. The interesting aspect of the blocked slip band model is the prediction (from equations (20) and (21)) that the long crack threshold K_0 increases with grain size, whereas the short crack threshold, or fatigue limit σ_e, decreases.[76] Such predictions are borne out by experiment and highlight the fact that metallurgical factors which may improve resistance to the growth of long cracks (i.e. raise ΔK_0) may simultaneously lower resistance to the initiation and growth of small cracks (i.e. lower $\Delta\sigma_e$).[77] This effect is particularly pronounced in ferrous alloys: as shown in Fig. 18, increasing the tempering temperature to decrease strength level in an ultrahigh strength, silicon modified 4340 steel (300M) lowers the long crack threshold ΔK_0, yet raises the fatigue limit $\Delta\sigma_e$ (Ref. 6). A second example, shown in Fig. 19, is from the work of Usami and Shida,[59] who compared the threshold behaviour as a function of surface roughness (to simulate crack size) of a cast iron (σ_0 = 113 MNm^{-2}) and a maraging steel (σ_0 = 1906 MNm^{-2}). It is quite clear from this work[59] that the maraging steel, while of substantially higher strength and having a far superior fatigue resistance at short crack sizes (below 0.1–1 mm), is actually inferior to cast iron from the viewpoint of long crack threshold behaviour.

Local plasticity effects

The second definition of a short crack (*see* the introductory section) refers to cracks which are of a size comparable to the scale of local plasticity, such as the crack tip plastic zone

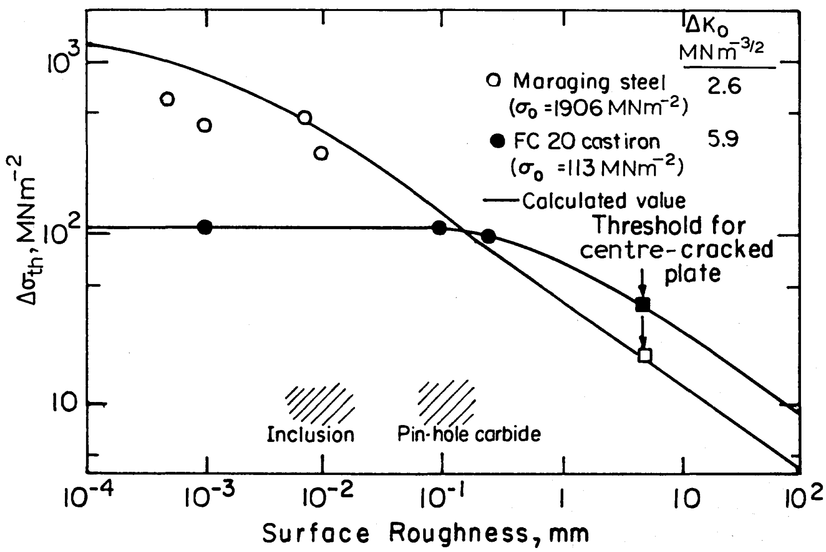

19 **Comparison of threshold behaviour of cast iron, σ_0 = 113 MNm^{-2}, and maraging steel, σ_0 = 1906 MNm^{-2}, as function of surface roughness (to simulate crack size)[59]**

generated by the crack itself (near-tip plasticity), or the strain field of a notch or a larger stress concentration which may encompass the crack in the vicinity of the notch (notch field plasticity). Each of these two local plasticity effects is examined below.

Near-tip plasticity effects

While elastic–plastic fracture mechanics analyses seem more suited to the characterization of short cracks comparable in size to the extent of self-induced near-tip plasticity, a comparison of their behaviour with equivalent long cracks using LEFM analyses (i.e. at the same nominal value of ΔK) shows that the short cracks grow much more quickly.[8–10,12,47,84] Part of the reason for such apparently anomalous results lies not in any physical difference between the behaviour of long and short cracks, but with the inappropriate use of LEFM analyses. This was shown particularly clearly by Dowling,[51] who monitored the growth of small surface cracks in smooth bar specimens of A533B nuclear pressure vessel steel subjected to fully reversed strain cycling. By analysing the growth rates da/dN in terms of ΔJ, using values of J computed from the stress–strain hysteresis loops (described by equation (17) and shown in Fig. 5), there was found a closer correspondence between the behaviour of long and short cracks (Fig. 20). Analogous approaches to the short crack problem have been suggested in terms of ΔK_ϵ, the pseudo-elastic–plastic strain intensity range,[85–87] or ΔK_{eq}, the equivalent stress intensity range,[87]

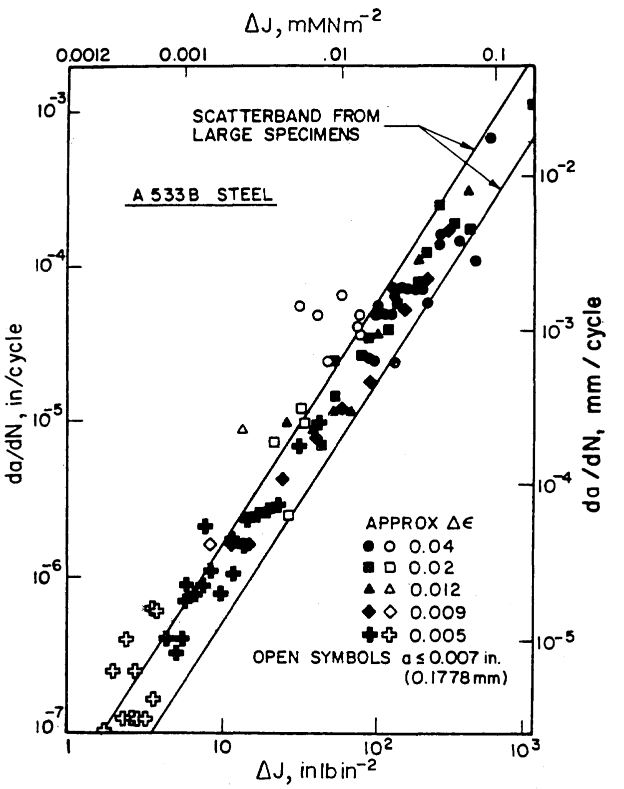

20 Variation of fatigue crack growth rates da/dN for long ($a \gtrsim 25$ mm) and short ($a \lesssim 0.18$ mm) cracks in A533B steel, $\sigma_0 = 480$ MNm^{-2}, under plastic loading; data analysed in terms of ΔJ (Ref. 51)

given in terms of a crack length a, elastic modulus E, and representative strain range $\Delta\epsilon$ as

$$\Delta K_\epsilon = \Delta\epsilon(\pi a)^{1/2} = (q\Delta\epsilon_e + \Delta\epsilon_p)(\pi a)^{1/2} \quad (22)$$

$$\Delta K_{eq} = QE\Delta\epsilon(\pi a)^{1/2} \quad (23)$$

where $\Delta\epsilon$ is the sum of the plastic strain range $\Delta\epsilon_p$ plus part of the elastic strain $q\Delta\epsilon_e$, where $0.5<q<1$, and Q is the compliance function based on the equivalent linear elastic K_I solution for the loading geometry in question. Recently, Starkey and Skelton[88] have shown that the ΔJ and ΔK_{eq} approaches are essentially the same up to high plastic strains, and good correlations have been found between data for long and short cracks at both room and elevated temperatures by expressing the crack growth data in terms of $(E\Delta J)^{1/2}$ or ΔK_{eq}.

Although analyses of the behaviour of short cracks in terms of elastic–plastic constitutive laws often seem necessary, even with the more appropriate characterization afforded by such fracture mechanics, it is still often apparent that short cracks propagate at somewhat faster rates (Fig. 20). In order to account for this further 'breakdown' in continuum mechanics characterization, El Haddad and co-workers[9,84,89,90] have proposed an empirical approach based on the notion of an intrinsic crack length parameter, a_0. These authors redefined the stress intensity factor in terms of the physical crack length plus a_0, such that the stress intensity range which characterizes the growth of fatigue cracks, independent of crack length, is given by the equation

$$\Delta K = Q\Delta\sigma^\infty[\pi(a + a_0)]^{1/2} \quad (24)$$

where Q is the usual geometry factor.[84] The 'material-dependent constant' a_0 was estimated from the limiting conditions of crack length where the nominal stress $\Delta\sigma^\infty$ approaches the fatigue limit $\Delta\sigma_e$ when $a \to 0$ and where $\Delta K = \Delta K_0$, i.e.

$$a_0 \approx \frac{1}{\pi}\left(\frac{\Delta K_0}{\Delta\sigma_e}\right)^2 \quad (25)$$

The value of the intrinsic crack size a_0 can be seen to be equivalent to the critical crack size above which ΔK_{th} becomes constant at the long crack threshold stress intensity ΔK_0 in Figs. 15 and 18. In other words, a_0 is an indication of the smallest crack size that can be characterized at the threshold in terms of LEFM. This intrinsic crack size approach has been claimed to be a special case of Tanaka and co-workers' blocked slip band model[76] discussed above, where the friction stress $\sigma_{fr}^\star$ in equation (20) is taken to be zero. Although somewhat physically unrealistic, setting $\sigma_{fr}^\star = 0, K_0 = K_c^m$, and $a_0 = w_0$ in equations (18) and (19) gives[76]

$$\sigma_{th} = \frac{K_0}{[\pi(a + a_0)]^{1/2}} \quad (26)$$

$$K_{th} = \frac{K_0\, a^{1/2}}{(a + a_0)^{1/2}} \quad (27)$$

which are identical to the expressions derived by El Haddad *et al.*[84] In equations (26) and (27), a_0 is essentially a fitting parameter that reproduces the variation of $\Delta\sigma_{th}$ with crack length shown in

Fig. 18. Furthermore, by recomputing both ΔJ and ΔK to include a_0, El Haddad *et al.*[91] have reanalysed the short crack data obtained by Dowling[51] (*see* Fig. 20) and claimed a closer correspondence between results for long and short cracks. This intrinsic or 'fictitious' crack size approach has also been used to characterize a short crack emanating from a notch,[64,91] as discussed in the next section.

Although such an approach is successful in explaining differences in the growth rate kinetics of long and short cracks obtained from conventional LEFM analyses, it is totally empirical, as the physical significance of the parameter a_0 is not understood; neither is there any convincing correlation between a_0 and any characteristic microstructural dimension.

A somewhat different approach to rationalizing the behaviour of long and short cracks, specifically with respect to the threshold condition, was adopted by Usami and co-workers.[59,92–94] To replace the notion that the threshold condition is one of constant stress for short cracks, but one of a constant stress intensity range for long cracks, these authors proposed a single criterion that the cyclic plastic zone dimension (r_Δ) at the fatigue limit is a material constant.[59,92–94] They used the Dugdale solution to approximate the size of this plastic zone at the fatigue limit ($r_\Delta{}^F$) for $R \geqslant 0$, in terms of the yield stress σ_0 and crack size a, i.e.

$$r_\Delta{}^F = a[\sec(\pi\Delta\sigma_{th}/4\sigma_0) - 1] \quad . \quad . \qquad (28)$$

which was shown to reproduce the form of the curve of $\Delta\sigma_{th}$ versus crack size shown in Figs. 15, 18, and 19. Similar to the model based on an intrinsic crack size, this model can again be considered a special case of the blocked slip band model (equations (18)–(21)) by setting $K_c^m = 0$ (Ref. 76). By developing similar expressions for negative R ratios, Usami and Shida[59] have also claimed to have explained the effects of stress ratio and yield strength on the behaviour of short cracks. However, experimental confirmation of the constancy of $r_\Delta{}^F$ at the threshold for long and short cracks and the validity of the Dugdale solutions for the size of the plastic zone in this instance has yet to be obtained.

Notch field plasticity effects

Local plasticity also has an important influence on the initiation and growth of cracks emanating from notches. Such cracks are defined as being short because their size is comparable to the extent of the strain field of the notch tip plastic zone (*see* Fig. 21).

Stress analyses and failure predictions for notched components have traditionally involved the use of theoretical elastic stress concentration factors k_t or, where plasticity is considered, procedures such as those developed by Neuber.[95] For example, the well-known Neuber rule suggests that the elastic stress concentration factor k_t, under conditions of plastic deformation, is given approximately by the geometric mean of the stress and strain concentration factors, k_σ and k_ϵ, respectively:[95]

$$k_t = (k_\sigma k_\epsilon)^{1/2} \quad . \quad . \quad . \quad . \quad . \quad . \quad . \qquad (29)$$

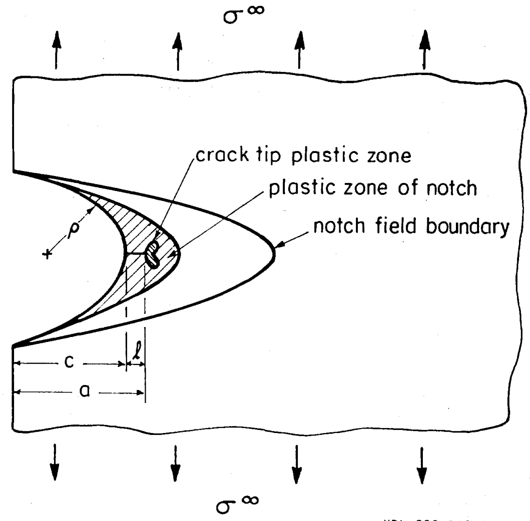

21 Schematic illustration of crack tip and notch tip plastic strain fields associated with growth of short crack of length l emanating from notch of depth c and root radius ρ

For elastic conditions, equation (29) reduces to

$$k_t = (\sigma\epsilon E)^{1/2}/\sigma^\infty \quad . \quad . \quad . \quad . \quad . \quad . \qquad (30)$$

where σ and ϵ are the local stress and strain at the notch surface, respectively, σ^∞ is the nominal applied stress, and E is the elastic modulus.

Although elastic stress concentration factors are sometimes used in fatigue for conservative design in the presence of notches, k_t is generally replaced by k_f, the fatigue strength reduction factor; k_f can be considered as the effective stress concentration under fatigue loading conditions and is defined for finite life as

$$k_f = \frac{\text{unnotched bar endurance limit}}{\text{notched bar endurance limit}} \leqslant k_t \qquad (31)$$

Values of k_f approach the theoretical values of k_t for larger notches and in higher strength materials, the degree of agreement being measured in terms of the so-called notch sensitivity index, defined as $(k_f - 1)/(k_t - 1)$. Although values of k_t are tabulated in handbooks (*see* e.g. Ref. 96), the determination of k_f generally involves experimental measurements or empirical predictions, such as the Peterson equation for iron-base wrought alloys,[97]

$$k_f \approx 1 + (k_t - 1)/[1 + (\alpha/\rho)] \quad . \quad . \qquad (32)$$

where ρ is the notch root radius and α is an empirical constant that depends on the strength and ductility of the material. Typical values for α range from 0.01 for annealed steels to 0.001 for highly hardened steels.[2] Since such empirical equations are available only for steels, to avoid always measuring k_f experimentally the so-called 'local strain approach', essentially a modification of the Neuber rule for cyclic loading, has recently been developed (*see* e.g. Refs. 2, 98, 99). The values of k_f suggested by Morrow and co-workers[98] are determined from the relations

$$k_f = (k_\sigma k_\epsilon)^{1/2} \qquad \text{(plastic)} \quad . \qquad (33)$$

$$k_f = (\Delta\sigma\Delta\epsilon E)^{1/2}/\Delta\sigma^\infty \qquad \text{(elastic)} \quad . \qquad (34)$$

where $\Delta\sigma^{\infty}$, $\Delta\sigma$, and $\Delta\epsilon$ are the ranges of the nominal stress, local stress, and local strain, respectively. To compute k_f, equation (34), which is the equation of a rectangular hyperbola ($\Delta\sigma\Delta\epsilon$ = constant), must be solved simultaneously with the cyclic constitutive law, which similarly relates cyclic stresses to cyclic strains.

Fracture mechanics analyses, incorporating both analytical and numerical procedures (e.g. from equations (7) and (8)) have also been utilized by many authors to treat the problem of notches in fatigue. In particular, Barsom and McNicol,[37] Smith and Miller,[100] Dowling,[21,101] Kitagawa,[102] Lukáš and Klesnil,[103] El Haddad and co-workers,[91,104,105] and Tanaka and Nakai[64] have all attempted to characterize the growth of small cracks which are either fully or partially submerged in a notch tip plastic zone. Although not concerned specifically with the growth of short cracks, Barsom and McNicol[37] proposed the concept of a fatigue crack initiation threshold $\Delta K/\rho^{1/2}$, which is assumed to be a material constant for the initiation of 'engineering sized' cracks from notches of different root radii ρ (*see* Fig. 22). With the usual definition of the stress concentration factor k_t, however, the concept of an initiation threshold $\Delta K/\rho^{1/2}$ is really the notched bar fatigue limit $\Delta\sigma_e k_t$ expressed in fracture mechanics terms.[7] Smith and Miller,[100] on the other hand, assumed that a fatigue crack of length a growing in an unnotched specimen is comparable to a fatigue crack of length l growing from a notch when both have the same instantaneous velocity under identical conditions of bulk applied stress. They further suggested that the contribution e ($= a - l$) to a crack of length l growing from an edge notch of depth c and root radius ρ can be expressed as

$$e = 7.691\, l(c/\rho)^{1/2} \quad . \quad . \quad . \quad . \quad . \quad (35)$$

and that the extent of the notch field is equal to $0.13(c\rho)^{1/2}$. This estimate of the size of the notch field appears to be less accurate for fairly sharp notches, and is in disagreement with the predictions made by Dowling[21] for this regime (equation (9)).

An interesting aspect of crack growth from notches is that, after growing a short distance, cracks can arrest completely and become so-called non-propagating cracks (NPCs), as first demonstrated by Phillips,[106] Frost,[107] and Frost and Dugdale.[108] Since then, a number of other studies[64,89,91,100,103,109–111] have confirmed that NPCs exist, although the mechanism(s) by which a propagating crack becomes an NPC is not understood. Stress–strain/life analyses, however, have revealed that NPCs form only at sharp notches, above the critical stress concentration factor k_t (*see* e.g. Refs. 100, 109, 111). This is illustrated in Fig. 23, where the long life fatigue strengths (i.e. fatigue limits) are plotted as functions of k_t. It is apparent from this figure that the threshold stress for crack initiation, i.e. the unnotched fatigue limit $\Delta\sigma_e$ divided by k_f or k_t, is less than the stress that would cause complete failure above the critical k_t for NPCs.

Fracture mechanics analyses of the plasticity of the notch field suggest that the condition for non-propagation involves either the long crack threshold stress intensity ΔK_0 applied to the short crack,[94] or a threshold strain intensity factor incorporating an intrinsic crack length (a_0) term.[89] As discussed below, the above models fail to explain physically why NPCs occur since the mere presence of a notch plastic zone does not obviously give rise to a driving force for crack growth which passes through a minimum.

Whether short cracks emanating from notches arrest or not, their growth, as compared to results obtained from conventional LEFM analyses of long cracks, is generally non-unique and significantly faster when characterized in terms of ΔK or K_{max}. An example of this behaviour is shown in Fig. 24, from the work of Leis and Forte,[110] where growth rates are plotted for cracks $\leq$250 μm long propagating from notches of varying k_t, and compared to the growth rates of long cracks in an SAE 1015 mild steel. Hammouda and Miller[109] have analysed such behaviour in terms of notch plasticity theory, and argue that the total plastic shear displacement, which is taken as the sum of the shear displacement arising from (notch) bulk plasticity and from the local crack tip plastic zone for LEFM controlled growth, determines the growth

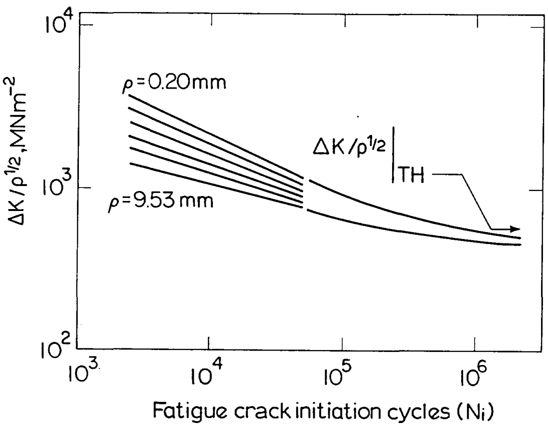

22 Correlation of fatigue life, based on initiation of engineering sized crack, with so-called fatigue crack initiation threshold $\Delta K/\rho^{1/2}$ based on results for HY130 steel, σ_0 = 1000 MNm^{-2}, double edge notched specimens of root radius ρ between 0.2 and 9.5 mm (Ref. 37)

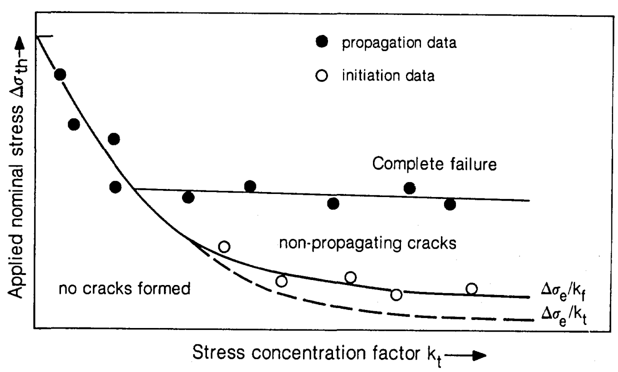

23 Threshold stress for crack initiation, i.e. unnotched fatigue limit $\Delta\sigma_e$ divided by k_f or k_t, as function of k_t (Ref. 111)

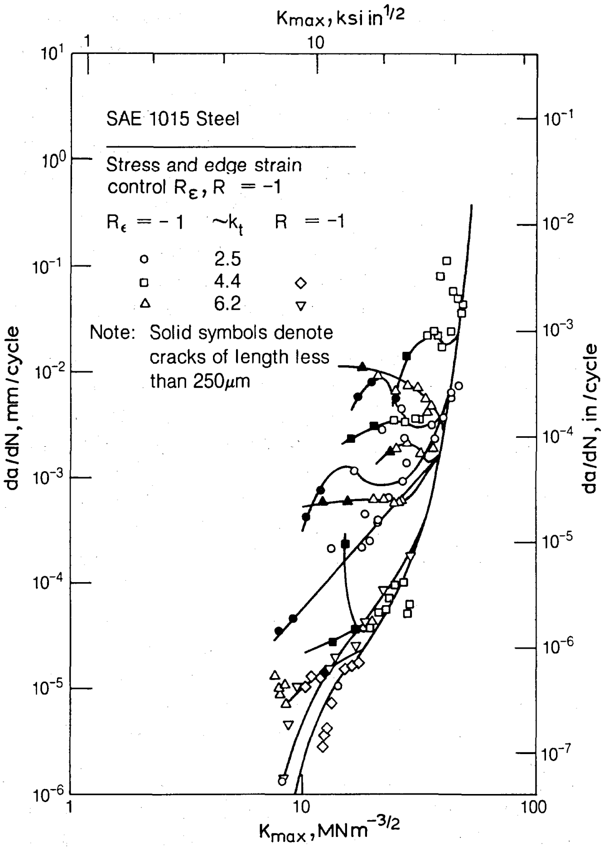

24 Propagation rate da/dN of cracks emanating from notches as function of maximum stress intensity factor K_{max} in 0.15%C mild steel; k_t is theoretical elastic stress concentration factor, R stress ratio, and R_ϵ edge strain ratio[110]

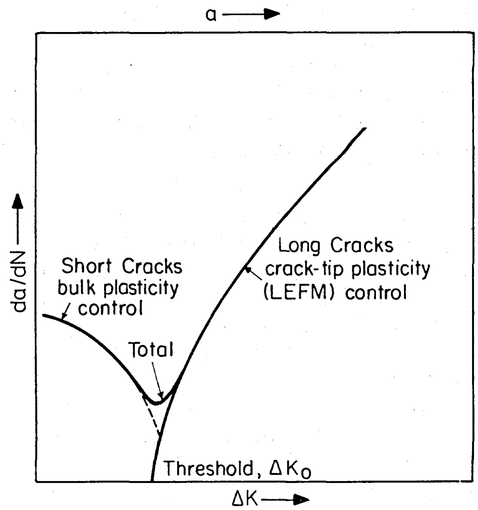

25 Elastic–plastic and linear elastic characterization of kinetics of crack growth for short crack propagation from notch, as shown in Fig. 21 (Ref. 109)

kinetics of such short cracks. If the crack is completely submerged in the notch tip plastic zone (*see* Fig. 21), bulk plasticity conditions dominate the behaviour. Hammouda and Miller estimate that the growth rates of the short cracks will decrease progressively until they arrest or merge with the long crack LEFM curve, where behaviour is dominated by local plasticity conditions within the crack tip plastic zone (*see* Fig. 25). Several continuum mechanics explanations have been advanced for such observations of growth rates of short cracks decreasing within the notch tip plastic zone. These explanations have been based on the total plastic shear displacement argument (*see* above),[109] on elastic–plastic analyses using the J parameter and the a_0 concept,[89] and on the idea that the size of the reversed plastic zone is a property of the material and is independent of crack length.[94] Such behaviour, however, is difficult to comprehend, particularly since there is a striking similarity between Figs. 25 and 14. In Fig. 14 is shown the progressive deceleration in short crack growth rates in the absence of a notch, which has been attributed to the impedance of growth at grain boundaries.[71] Thus it must be concluded that even though the precise mechanism for the deceleration of short crack growth and the formation of NPCs is unclear, factors such as notch tip plasticity, microplasticity, grain boundary blocking of slip bands, cessation of growth, crystallographic reorientation, deflection at grain boundaries, and crack closure may all play a significant role. In this regard it has been claimed that, since small cracks are capable of propagating below the long crack threshold ΔK_0 value, they may propagate for some distance until the combination of their size and the local stress causes them to arrest at or below the ΔK_0 value.[8] Although this is a convenient explanation of the behaviour shown in Figs. 14 and 25, the physical mechanisms that have been suggested for such behaviour do not follow from conventional elastic or elastic–plastic notch analyses. However, recent studies have suggested that the most general explanation involves the phenomenon of fatigue crack closure, and the variation of closure with crack length.[12,61] This is discussed in detail below.

Environmental and closure effects

The third definition of a short crack (*see* the introductory section), perhaps the most important from a design viewpoint, is the crack which is long compared to the scale of both the microstructure and the local plasticity, yet simply physically small, i.e. typically less than 0.5–1 mm long. Since both continuum mechanics and LEFM characterizations of the behaviour of such cracks would be expected to be valid, it is perhaps surprising to find that under certain circumstances[11,48,49,54,60] even physically short cracks grow faster than long cracks under a nominally identical driving force (i.e. at the same ΔK). This is not at all consistent with the concept of similitude, which forms the basis of fracture mechanics analyses of subcritical crack growth, and has been attributed primarily to two factors.[32]

The first of these is connected with the phenomenon of crack closure: interference and physical contact between mating fracture surfaces in the wake of the crack tip can, under positive loads during the fatigue cycle, lead to effective

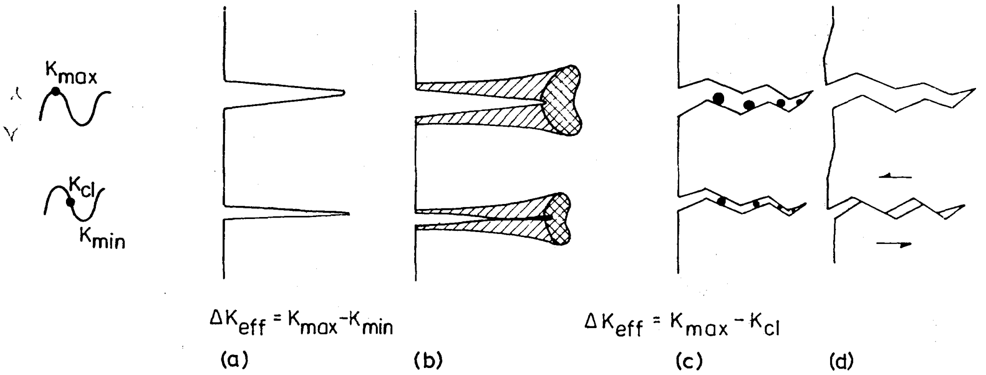

a no closure, and closure induced by: *b* cyclic plasticity; *c* corrosion deposits; *d* rough fracture morphology

26 Mechanisms of fatigue crack closure; ΔK_{eff} is effective stress intensity range, defined by $K_{max} - K_{cl}$, where K_{cl} is stress intensity at which two fracture surfaces come into contact ($K_{cl} \geq K_{min}$) (Ref. 119)

closure of the crack. Since the crack cannot propagate while it remains closed, the net effect of closure is to reduce the nominal stress intensity range ΔK, computed as $K_{max} - K_{min}$ from measurements of applied load and crack length, to some lower effective value ΔK_{eff} actually experienced at the crack tip, i.e. $\Delta K_{eff} = K_{max} - K_{cl}$, where K_{cl} is the stress intensity at closure ($\geq K_{min}$).[112] Several factors can lead to closure, such as the constraint of surrounding elastic material on the residual stretch in material elements previously plastically strained at the tip (plasticity induced closure),[112] the presence of corrosion debris within the crack (oxide induced closure),[113–116] and contact at discrete points between faceted or rough fracture surfaces where significant inelastic mode II crack tip displacements are present (roughness induced closure).[116–120] These mechanisms of crack closure are illustrated schematically in Fig. 26.

Plasticity induced closure, as first defined by Elber[112] from compliance measurements on fatigue cracks in aluminium alloys at high stress intensity ranges, is generally considered to play a dominant role under plane stress and is thus presumed to be of less importance at near-threshold levels where mostly plane strain conditions exist. In the latter case, the main contributions to the closure of fatigue cracks come from oxide deposits within the crack and from premature contact between the fracture surface asperities. Consideration of simple geometric models have led Suresh, Ritchie, and co-workers[119–122] to propose the following relationships for such closure:

$$(K_{cl}/K_{max})_{oxide} \approx (d_0^2\ \beta/\pi s \delta_{max} \epsilon_0)^{1/2} \qquad (36)$$

$$(K_{cl}/K_{max})_{roughness} \approx [2\gamma x/(1 + 2\gamma x)]^{1/2} \qquad (37)$$

where d_0 is the maximum thickness of the excess oxide deposit located a distance $2s$ from the crack tip, δ_{max} is the maximum CTOD (mode I), x is the ratio of mode II to mode I crack tip displacements, ϵ_0 is the yield strain (σ_0/E), γ is a non-dimensional roughness factor given by the ratio of the height of a fracture surface asperity to its width, and β is a constant of numerical value ~1/32.

Extensive studies of the behaviour of long cracks, particularly at near-threshold stress intensity levels, have revealed that such closure mechanisms determine to a large extent the effects on crack growth of load ratio,[114–116,123] yield strength,[116,124,125] grain size,[116,120] environment,[114–116,121,122,125] and variable amplitude cycling,[126–128] and even in the very existence of a threshold for no long crack growth.[116,121,125,129] However, such microscopic closure mechanisms are also particularly relevant to the behaviour of short cracks, simply because their action predominates in the wake of the crack tip. Since small cracks, by definition, have only a limited wake, it is to be expected that the effect of crack closure will be different for long and short cracks — that the short crack is likely to be less influenced by closure. Evidence that the extent of crack closure is a function of crack size has been reported by James and Morris[48] for the growth of short cracks in titanium alloys. By monitoring the surface CTOD at zero load for cracks from 50 to 500 μm long (*see* Fig. 27), these authors concluded that for cracks less than approximately 160 μm long the extent of crack

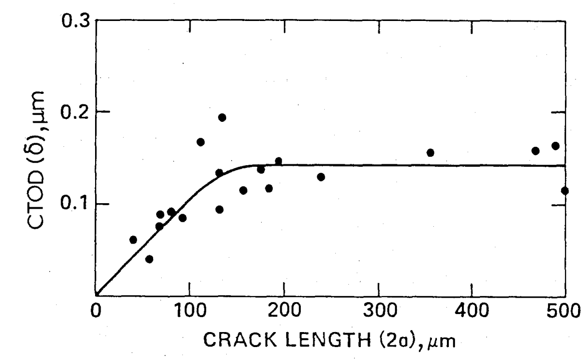

27 Variation of CTOD δ at zero load with length of small surface cracks in 6Al–2Sn–4Zn–6Mo titanium alloy (σ_0 = 1140 MNm^{-2}, primary α grain size ≈ 4 μm, β grain size ≈ 12 μm), showing reduction in crack closure with decreasing crack size[48]

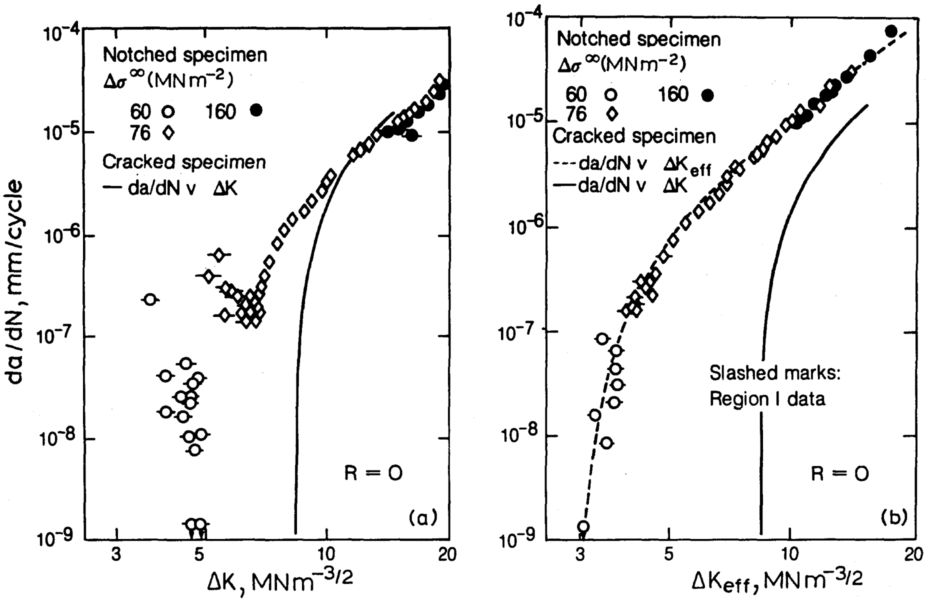

a da/dN *v*.nominal stress intensity range ΔK; *b* da/dN *v*.effective stress intensity range ΔK_{eff}, note that anomalous (sub-threshold) behaviour of short cracks is brought into direct correspondence with conventionally obtained data for long cracks once crack closure is accounted for

28 Variation of crack propagation rate with stress intensity ranges in JIM SM416, 0.17%C structural mild steel, σ_0 = 194 MNm^{-2} (Ref. 61)

closure, particularly that induced by roughness, decreased with decreasing crack length. A further influence of roughness-induced closure was found by McCarver and Ritchie,[60] who studied the crystallographic growth of long and physically short fatigue cracks in René 95 nickel-base superalloy. Threshold ΔK_{th} values for short cracks (a~0.01–0.20μm) at low mean stresses (R = 0.1) were found to be 60% smaller than for long cracks (a~25 mm), yet at high mean stresses (R = 0.7) where closure effects were minimal, this difference was not apparent. More recently, Tanaka and Nakai[61] have used compliance techniques to measure the extent of crack closure for small cracks emanating from notches in a low carbon steel and found a marked reduction in closure at short crack lengths. These authors claimed that the anomalous (sub-threshold) behaviour of short cracks (as shown in Figs. 14 and 25) could be brought into direct correspondence with conventional long crack data (*see* the next section) by analysing it in terms of ΔK_{eff} (*see* Fig. 28). Thus, at equivalent nominal ΔK levels, physically short cracks may be expected to propagate faster (and show lower thresholds) than corresponding long cracks simply because closure produces a smaller increase in effective stress intensity range at the crack tip in long cracks. Specific mechanisms for this effect are discussed in more detail in the next section.

Chemical and electrochemical effects can also increase the growth rate of small cracks, and this is particularly relevant to the growth of physically short cracks in aggressive environments.[11,53,54,57,130] Experiments by Gangloff[11,54] on high strength AISI 4130 steels tested in NaCl solution revealed the corrosion fatigue crack propagation rates of short cracks (0.1-0.8 mm) to be up to two orders of magnitude faster than corresponding rates for long cracks (25–60 mm) at the same ΔK level, although the behaviour in inert atmospheres was essentially similar (see Fig. 29). This phenomenon is not completely understood, but preliminary analyses have indicated that the effect could be attributable to differences in the local crack tip environment of long and short cracks, resulting mainly from the different electrochemically active surface-to-volume ratios of the cracks and from the influence of crack length on the solution renewal rate in the crack tip region.[11,54,57]

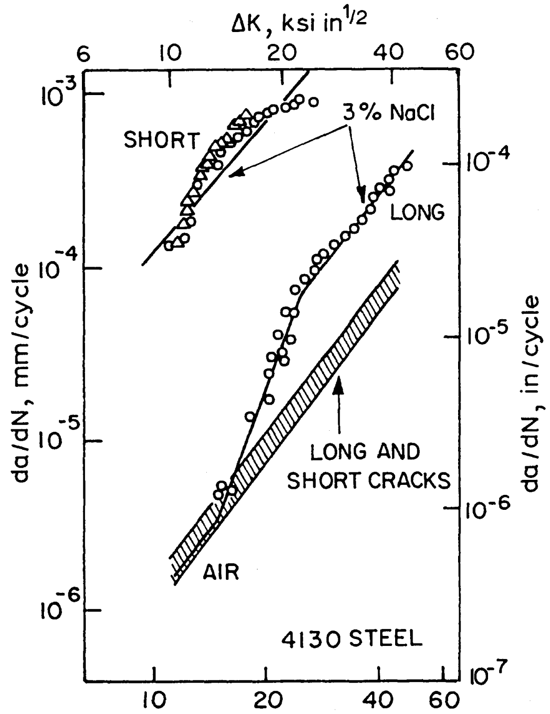

29 Fatigue crack propagation rate da/dN as function of ΔK for long (a ~ 50 mm) and physically short (a = 0.1–0.8 mm) cracks in AISI 4130 steel, σ_0 = 1300 MNm^{-2}, tested in moist air and in aqueous 3% NaCl solution[53]

DISCUSSION

From the above review of experimental results, it is apparent that short fatigue cracks may present difficulties in fatigue design simply because their growth behaviour cannot be predicted with certainty by using the analyses and methodologies developed for long cracks, for example by making use of LEFM results. It is also apparent that the use of these procedures can lead to overestimates of the lifetimes of components containing short cracks because, under the same nominal driving force, a short crack invariably propagates more quickly than a corresponding long crack. This problem, of 'lack of similitude', arises for a number of reasons, including:

(i) inappropriate fracture mechanics characterization of the crack driving force for short cracks subjected to near-tip and notch field plasticity effects
(ii) local microstructural features which do not substantially alter the growth of large cracks, but can interact strongly with small cracks because they are of comparable size
(iii) lack of similitude associated with crack extension mechanisms
(iv) crack closure effects
(v) differences in the local crack tip environments.

Each of these factors is now examined in turn.

Questions on the inappropriate use of LEFM to characterize the extension of short cracks have been central to the short crack problem (*see* e.g. Refs. 7–10, 12, 131, 132). In fact, it has often been claimed that the short crack problem arises simply when LEFM analyses become invalid,[131] although it is now clear that this is an oversimplification. Conventional LEFM approaches can be inappropriate for short cracks, even under nominally elastic conditions, since the use of the linear elastic singularity to characterize the local stresses on the basis of K_I (i.e. equation (3)) invariably involves neglecting all terms of order higher than $r^{-1/2}$ (Ref. 133 and 134). However, when $a \sim r_y$ such higher order terms can have an appreciable effect and therefore should be considered when comparing the behaviour of long and short cracks.[133,134] It is also well recognized that one of the main reasons for the breakdown in LEFM analyses for short cracks is the presence of excessive plasticity over distances comparable with the crack size in the vicinity of the crack tip. This problem has been partly resolved by the use of elastic–plastic fracture mechanics in methods based on the J-integral or on the crack tip opening displacement, as evidenced by the results obtained by Dowling[51] and shown in Fig. 20. It is now apparent that differences in the behaviour of long and short cracks as revealed by early studies can be traced to the fact that growth rates were compared at equivalent ΔK values, and that the use of this LEFM parameter did not provide an adequate characterization of the stress and strain fields at the tip of short cracks, where $a \sim r_y$. However, for short cracks emanating from notches, where initial growth occurs within the plastic zone of the notch (*see* Fig. 21), a continuum mechanics description of the behaviour is less clear. Certainly there is experimental evidence that such short cracks can propagate below the long crack threshold at progressively decreasing growth rates (*see* Fig. 25), and can even arrest to form non-propagating cracks,[106–110] but such behaviour can also occur in the absence of a notch and can be attributed to microstructural factors (*see* Fig. 14).[71] Certainly no linear elastic analysis of a short crack emanating from a notch (*see* e.g. Refs. 21, 100) has shown that the crack driving force (e.g. K_I) passes through a minimum as the crack begins to extend from the notch, and to the present authors' knowledge there is no formal elastic–plastic analysis available which predicts a similar variation in crack driving force without having to incorporate crack closure effects.[12,64,135] Although there is no complete continuum mechanics analysis, it can be concluded that the anomalous growth rate of short cracks emanating from notches may result in part from the interaction of the short crack with microstructural features, and principally from crack closure.

With respect to microstructural features, it is generally accepted that the presence of microscopic discontinuities, such as grain boundaries, hard second phases, or inclusions, plays a somewhat minimal role in influencing the growth of long fatigue cracks[6] (at least for growth rates below ~10^{-3} mm/cycle) because the behaviour is governed primarily by average bulk properties.[10] However, it is clear that this is not the case for small cracks whose length is comparable to the size of microstructural features. For example, for small cracks contained within a single grain, cyclic slip will be strongly influenced by the crystal orientation and the proximity of the grain boundary, resulting in locally non-linear crack extension.[49,71–74] There is now a large body of evidence showing that the growth of small cracks is impeded by the presence of grain boundaries (*see* e.g. Fig. 30) by such mechanisms as the blocking of slip bands[76] or containment of the plastic zone[49] within the grain, reorientation and reinitiation of the crack as it traverses the boundary,[49,71] and simple cessation of growth at the boundary.[49] Crack propagation has also been found to be halted by harder second phases: in duplex ferritic–martensitic steels, small cracks

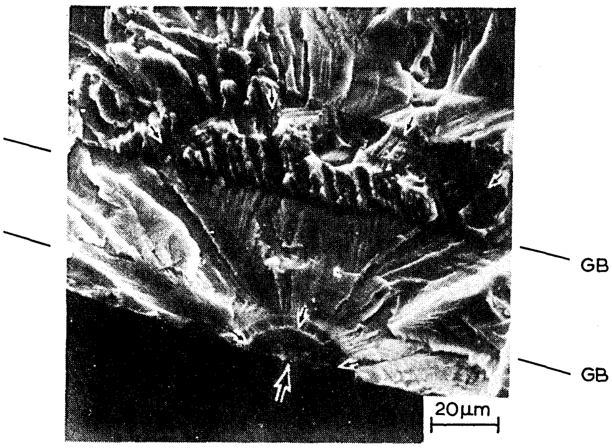

30 Changes in direction of crack advance when crack tip encounters grain boundaries in 7075 T6 aluminium alloy[71]

were observed to initiate and grow in the softer ferrite, only to arrest when they encountered the harder martensite.[136] Many of these effects can be explained by considering the mechanics of crack deflection.

Based on the theoretical analyses by Bilby *et al.*[137] and Cotterell and Rice,[138] recent studies by Suresh[81] have shown that alternatives to previous interpretations of the way in which a crack tip interacts with a grain boundary can be developed by considering the effect of crack deflection on the propagation of short fatigue cracks. For a short crack, the low restraint on cyclic slip promotes a predominantly crystallographic mode of failure. When a crack tip reaches a grain boundary, it tends to reorient itself in the adjacent grain to advance by the single shear mechanism, and can be considerably deflected by the grain boundary. This phenomenon is illustrated schematically in Fig. 31. The extent of deflection at the grain boundary is a function of the relative orientations of the most favourable slip systems in the adjoining crystals. For an elastic crack initially inclined at an angle θ_0 to the mode I growth plane and deflected at the first grain boundary through an angle θ_1 (*see* Fig. 31), approximate estimates of the local stress intensity factors yield the relation[81]

$$K_1/K_I = \cos^2\theta_0 \cos^3(\tfrac{1}{2}\theta_1) + 3\sin\theta_0 \cos\theta_0 \sin(\tfrac{1}{2}\theta_1)\cos^2(\tfrac{1}{2}\theta_1) \quad . . . . . . (38)$$

$$K_2/K_I = \cos^2\theta_0 \sin(\tfrac{1}{2}\theta_1)\cos^2(\tfrac{1}{2}\theta_1) - \sin\theta_0 \cos\theta_0 \cos(\tfrac{1}{2}\theta_1)[1 - 3\sin^2(\tfrac{1}{2}\theta_1)] \quad . . . . . . (39)$$

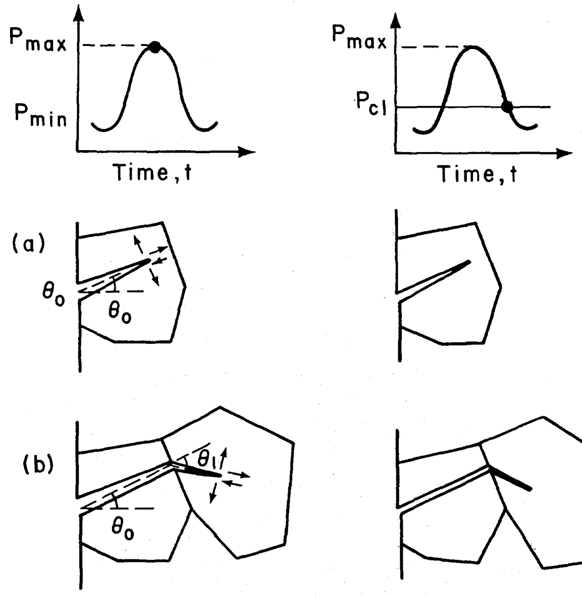

a propagation into first grain; *b* propagation across grain boundary

31 Growth and deflection of microstructurally short fatigue crack and the resultant crack tip displacements and closure; θ_0 is short crack initiation angle and θ_1 angle of deflection at first grain boundary[81]

Here, K_1 and K_2 are the near-tip mode I and mode II stress intensity factors, respectively, immediately following deflection at the grain boundary, whereas K_I is the nominal mode I (far-field) value. For a typical short crack emanating from the surface at an angle of $\theta_0 \approx 45°$ and deflected at the grain boundary by $\theta_1 \approx 90°$, equations (38) and (39) yield $K_1 \approx 0.7K_I$ and $K_2 \approx 0.35K_I$. The effective driving force for coplanar growth can then be approximated as the square root of the sum of the squares of K_1 and K_2, such that $\Delta K_{eff} \approx 0.78\Delta K_I$. Thus consideration of crack deflection processes alone can account for a significant reduction in driving force as a crack tip interacts with a grain boundary when the way in which a short crack advances is characterized by LEFM. It has been postulated[81] that if the extent of deflection at the grain boundary is large, the effective cyclic stresses may be reduced to a value smaller than the true threshold for short crack advance (e.g. to the fatigue endurance limit) such that complete crack arrest will result (denoted by curve A in Fig. 32). If the effective cyclic stresses after deflection are above such threshold values, there would be no crack arrest (as denoted by curve B in Fig. 32) and only a temporary deceleration in growth rate. Although the numerical predictions of the deflection models can be subject to considerable uncertainties when used to characterize the mechanics of short cracks in metals and alloys, the mechanisms underlying crack deflection processes have been shown to provide a physically meaningful explanation not only for the role of microstructure in influencing short crack advance, but also for several fatigue characteristics of long cracks under constant[81] and variable amplitude[81,126–128] loading.

In addition to causing a reduction in the effective driving force, crack deflection mechanisms could play a major role in enhancing closure.[81,120] For example, the irreversibility of

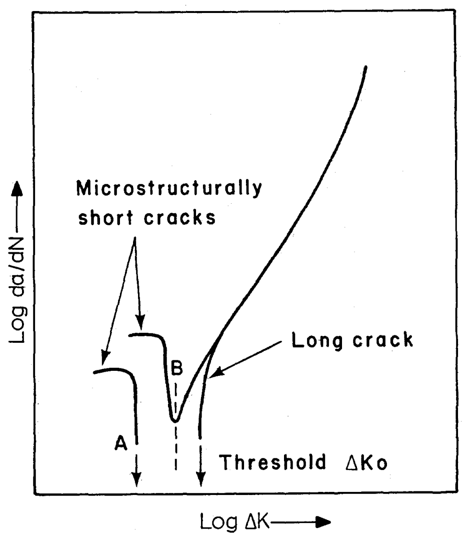

32 Variation of fatigue crack growth rate da/dN with ΔK for both long and microstructurally short fatigue cracks; note how growth rates for short cracks decrease progressively below long crack threshold ΔK_0 before arresting or merging with long crack data

slip steps and surface oxidation can lead to non-uniform tensile opening and shear displacements of short cracks.[12,81] Given the presence of serrated fracture surfaces and mode II crack tip displacements occurring after deflection, such non-uniformities in crack opening and sliding result in premature contact between asperities, leading to roughness induced closure (*see* Figs. 26 and 31). (An ideally elastic crack may not result in any roughness induced closure, irrespective of the extent of deflection.) Experimental measurements of crack closure made by Morris and co-workers[47–49] do indeed show that even short cracks (spanning only a few grain diameters) can close above the minimum load of the fatigue cycle (*see* Fig. 27).

A further factor which may contribute to differences in the behaviour of long and short cracks is the question of crack shape.[10] Even long cracks, running across many grains, are known to possess certain irregularities in their geometry (on a microscopic scale) that result from local interactions with microstructural features,[10] yet, at a given ΔK, the overall growth behaviour would be expected to be similar. However, on comparing a large crack with a small one this similarity would seem questionable. Moreover, the early stages of fatigue damage often involve the initiation of several small cracks, the subsequent growth of any of which is likely to be strongly influenced by the presence of the others.[37–40]

Differences in the behaviour of long and short cracks may also result from the fact that, at the same nominal ΔK, the crack extension mechanisms may be radically different. As pointed out by Schijve,[10] the restraint of the elastic surrounding on a small crack near a free surface is very different from that experienced at the tip of a long crack inside the material. For a small, grain sized crack, cyclic slip along the system with the highest critical resolved shear stress results in mixed mode II and mode I slip band cracking akin to Forsyth's stage I mechanism.[139] However, for a long crack, spanning many grains, maintaining such slip band cracking in a single direction in each grain is incompatible with maintaining a coherent crack front. The resulting increased restraint on cyclic plasticity will tend to activate further slip systems, leading to a non-crystallographic mode of crack advance by alternating or simultaneous shear, commonly referred to as striation growth (Forsyth's stage II).[139] At near-threshold levels where the extent of local plasticity can be small enough to be contained within a single grain, even long cracks may propagate via the single shear mechanism, the orientation of the slip band cracking changing at each grain boundary and leading to a faceted or zigzag crack path morphology (*see* Fig. 33).[117–120]

The occurrence of this shear mode of crack extension, with the related development of a faceted fracture surface, has a major influence on the magnitude of crack closure effects,[116–120] which may in turn lead to differences in the behaviour of long and short cracks (*see* Figs. 26 and 31).

The differences in fatigue characteristics resulting from crack closure arise from two main sources. First, since closure results from the constraint of surrounding elastic material on the plastic region surrounding the crack, the amount of closure experienced by a small crack at high stress amplitudes in a fully plastic specimen would be far less than that experienced by a larger crack at lower stress amplitudes in an elastic–plastic or nominally elastic specimen at the same (nominal) driving force. However, more importantly, differences between the effect of closure on long and short cracks result from the fact that such closure effects predominate in the wake of the crack tip. Since short cracks — by definition — possess a limited wake, it is to be expected that in general such cracks will be subjected to less closure. Thus, at the same nominal driving force, short cracks may experience a larger effective value than will the equivalent long crack. As outlined in the previous section, this can arise in two ways. In the first, with respect to plasticity induced closure, plastic deformation in the wake of the crack has to build up before it can be effective in reducing ΔK_{eff} (Ref. 112). From analogous studies of the role of dilatant inelasticity (inelasticity resulting from phase transformations) on reducing the effective stress intensity at the crack tip in ceramics,[140] it has been found that the full effect of this closure is felt only when the transformed zone extends into the wake of the crack by a distance of five times its forward extent. Although no comparable analysis has been carried out for plastic deformation in metals, it is to be expected that the role of the compressive stresses in the plastic zone encompassing the wake of the crack would be limited for small cracks of a length comparable to the forward extent of this zone (i.e. for $a \sim r_y$). It is believed[12,64,133] that this is one of the main reasons (at least from the perspective of continuum mechanics) for non-propagating cracks and also explains why microstructurally short cracks and cracks emanating from notches can propagate below the long crack threshold ΔK_0 (*see* Figs. 14 and 25). Essentially, they can initiate and grow at nominal stress intensities below ΔK_0 because of the absence of closure effects but, as they increase in length, the build-up of permanent residual plastic strains in their wake means that crack closure begins to have the effect of progressively decreasing the effective ΔK experienced at the crack tip, resulting in a progressive reduction in crack growth rate and sometimes complete arrest.

This notion, by which the anomalous behaviour of short cracks below the long crack threshold regime and in the strain field of notches (*see* e.g. Fig. 1) is related primarily to a decrease in crack closure effects at small crack sizes,[12,64,135] has recently been substantiated by both numerical[135] and experimental[64] studies. Newman[135] has demonstrated that by incorporating plasticity induced closure in finite element computational models of fatigue crack propagation, the progressively decreasing growth rates of short cracks emanating from notches could be predicted and shown to be in good agreement with experimental data on lower strength steel (*see* Fig. 34). Tanaka and Nakai[64] monitored the growth of similar short cracks in notched specimens of low strength steel at both $R = 0$ and 0.4 while simultaneously measuring the extent of crack closure. Their data, which

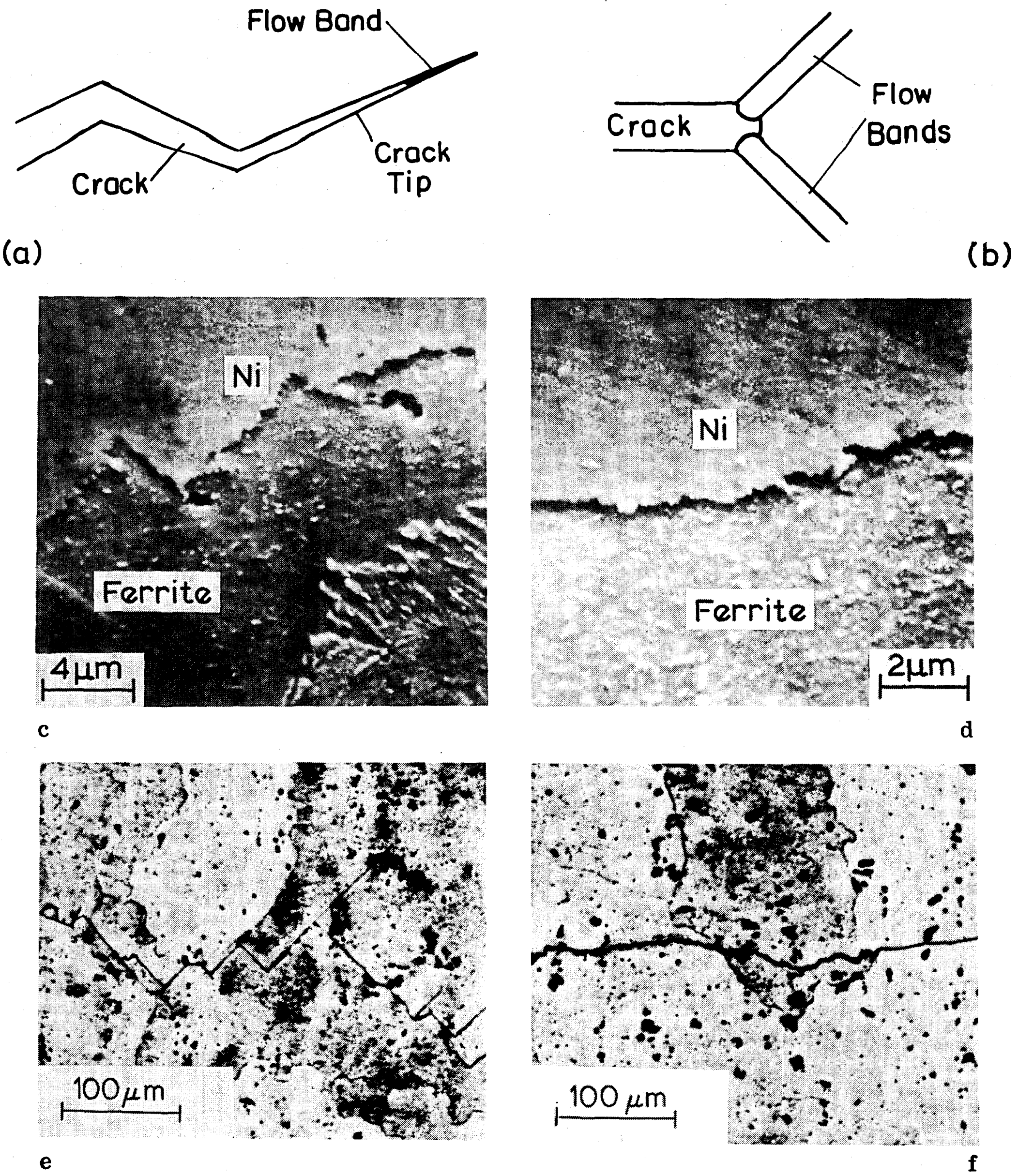

a, c, e near threshold, $r_y < d_g$, stage I, mixed modes I and II; *b, d, f* higher growth rates, $r_y > d_g$, stage II, mode I; *c, d*, fractographs of nickel-plated 1018 steel;[118] *e, f* sections of 7075 T6 aluminium alloy[10]

33 Crack opening profiles and morphologies of long fatigue cracks[120]

show the characteristic decreasing growth rate for short cracks when plotted in the usual way (in terms of a nominal ΔK), can be seen to coincide with the long crack data and to fall on a single smooth curve when reanalysed in terms of ΔK_{eff} incorporating the experimental K_{cl} measurements (*see* Fig. 28).

A similar situation can arise from the effect of roughness induced crack closure promoted by rough, irregular fracture surfaces, particularly if the crack extension mechanism involves a strong single shear (mixed mode II and mode I) component.[118-120] Since a crack of zero length can have no fracture surface and hence cannot undergo roughness induced closure, the development of such closure is expected to be a strong function of crack size,[47-49,120,133] as demonstrated by the experimental data obtained by James and Morris[48] and shown in Fig. 27. An estimate of the lower bound to the size of transition crack below which roughness induced closure is ineffective (at near-threshold levels) can be appreciated from Figs. 31 and 33 (Ref. 120). A long crack which encompasses several grains will, at near-threshold levels, have developed a faceted morphology and, as a result of the incompatibility between mating crack surfaces arising from the mode II crack tip displacements, will undergo roughness induced closure in the manner depicted in Fig. 26. The short crack, however, will not undergo such closure while its length remains less than a grain diameter since it will not have changed direction at a grain boundary, and accordingly will not have formed a faceted morphology, despite extension via the same single shear mechanism.

In general, since most of the results that show differences between the growth rates of long and short cracks have been obtained at low stress

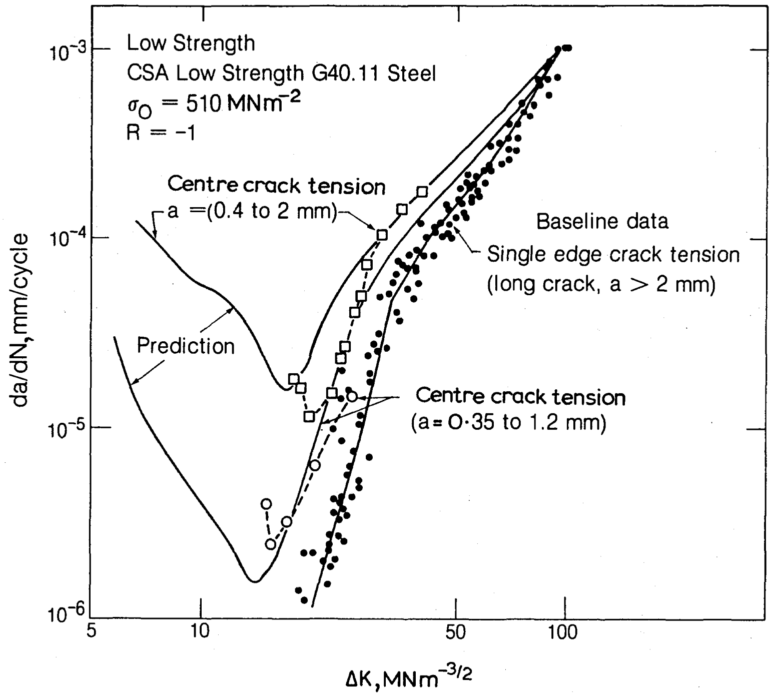

34 **Comparison of experimental results and numerical predictions of crack propagation rates for small cracks in centre cracked tensile specimens of CSA G40.11 low strength structural steel σ_0 = 510 MNm^{-2}, subjected to high stress levels[135]**

intensity ranges, and fatigue-crack propagation of long cracks in this near-threshold regime is known to be strongly influenced by crack closure effects, it seems most likely that the main reason for the faster growth of short cracks and the fact that they can propagate below the long crack threshold ΔK_0 is associated with the role of closure decreasing with crack size. Results obtained by Potter and Yee[141] on the behaviour of short cracks under variable amplitude loading are consistent with this notion, since the crack growth transients (i.e. accelerations and retardations) normally observed following overloads and spectrum loading sequences, which have been attributed — at least in part — to closure mechanisms (*see* e.g. Ref. 112), were largely absent for short cracks. In this regard it is useful to compare data for short and long cracks at high load ratios, since closure effects are then minimal even for long cracks. This has been done for crystallographic near-threshold fatigue in nickel-base alloys,[60] and the threshold for short cracks, despite being 60% smaller than the long crack threshold at $R = 0.1$, was approximately equal to the long crack threshold at $R = 0.7$.

Finally, large differences in the behaviour of long and short cracks can arise at stress intensities well outside the threshold regime, because of environmental factors.[11,54,130] As shown in Fig. 29, the results obtained by Gangloff[11,54] have demonstrated that corrosion fatigue crack growth rates of physically short cracks in AISI 4130 steel tested in aqueous NaCl solution can be one to two orders of magnitude faster than the corresponding growth rates of long cracks at the same ΔK value. This unique environmentally assisted propagation of short cracks was attributed to differing local crack tip environments as a function of crack size. Specifically, Gangloff argued that the local concentration of the embrittling species within the crack depends on the surface-to-volume ratio of the crack, on the diffusive and convective transport of the embrittling medium to the crack tip, and on the distribution and coverage of active sites for electrochemical reaction, all processes sensitive to crack depth, opening displacement, and crack surface morphology.[54,57] Analogous, yet less spectacular, environmental crack size effects may also arise in gaseous environments or in the presence of internally charged hydrogen where, for example, the presence of hydrogen may induce an intergranular fracture mode. The rough crack surfaces that tend to be produced by this failure mechanism would lead to roughness induced closure, which again directly influences the long crack phenomenon of a reduced ΔK_{eff} (*see* e.g. Ref. 142).

These differences in the behaviour of fatigue cracks of different size provide clear examples of how the fracture mechanics similitude concept can break down. The stress intensity, although adequately characterizing the mechanical driving force for crack extension, can account for neither the chemical activity of the crack tip environment nor the local interaction of the crack with microstructural features. Since these factors, together with the development of crack closure, are a strong function of crack size, it is actually unreasonable to expect the growth behaviour of long and short cracks to be identical. Thus, in the absence of the similitude relationship, the analysis and utilization of laboratory fatigue-crack propagation data to predict the performance of in-service components in which short cracks are present becomes an extremely complex task; a task which demands an immediate and major effort from both researchers and practising engineers alike.

CONCLUDING REMARKS

The problem of short cracks must be recognized as one of the most important and challenging topics currently faced by researchers in fatigue. Not only is it a comparatively unexplored area academically, but it also raises doubts about the universal application to the characterization of sub-critical flaw growth of fracture mechanics, the misuse of which can result in overestimates of defect-tolerant lifetimes. It is an area that, represents an interface between the fracture mechanics methodologies dealing specifically with the macroscopic growth of fatigue cracks and the classical engineering mechanics methodologies dealing with total life and engineering concepts of (macro-) crack initiation (as depicted in Fig. 1). As discussed in the introductory section, the last process, of macrocrack initiation, is simply the growth of short cracks (microcracks). The process of the initiation of short cracks (microcrack initiation) has not been treated explicity in this paper as it has been the subject of several recent reviews (*see* e.g. Refs. 7, 143, 144). Suffice it to say that such small cracks tend to initiate at constituent particles (i.e. inclusions and intermetallics, as shown in Fig. 9) in commercial materials (*see* e.g. Refs. 39, 41, 145), whereas in pure metals and alloys their initiation is often associated with emerging planar slip bands called persistent slip bands (PSBs) (*see* e.g. Ref. 143, 144, 146, 147). In fcc metals, such small cracks appear to initiate via a crystallographic stage I mechanism along the PSB, as shown in Fig. 35 (Ref. 148), although the specific mechanisms of initiation and their relation to the PSBs vary markedly from material to material.[144]

In the present paper an attempt has been made to provide a critical overview of recent experimental studies on the growth of small fatigue cracks, and specifically to outline the mechanical, metallurgical, and environmental reasons, as to why the behaviour of such cracks should differ from the behaviour of long cracks. The intention has not been to present a formal analysis of each of these factors, since in most cases such an analysis is simply not possible, but rather to give a thorough review of the many interdisciplinary factors which may be relevant to the short crack problem. It has been concluded that differences in the behaviour of short and long cracks are to be expected, and that such differences can arise from a number of distinct phenomena:

(i) inadequate characterization of the mechanics of crack tip stress and deformation fields of short cracks, including the neglect of higher order terms for the elastic singularity and the presence of extensive local crack tip plasticity
(ii) notch tip stress and deformation field effects (for cracks emanating from notches)
(iii) the interaction, including deflection, of short cracks with microstructural features such as grain boundaries, inclusions, and second phases, of dimensions comparable in size with the crack length
(iv) differences in crack shape and geometry
(v) differences in crack extension mechanism
(vi) the effect of crack closure varying with crack length
(vii) differences in the local crack tip environments.

Each of these factors represents a formidable challenge in fatigue research because of the complex nature of both experimental and theoretical studies, yet they are of great importance to an understanding of the anomalous behaviour of short flaws. This problem will undoubtedly come to

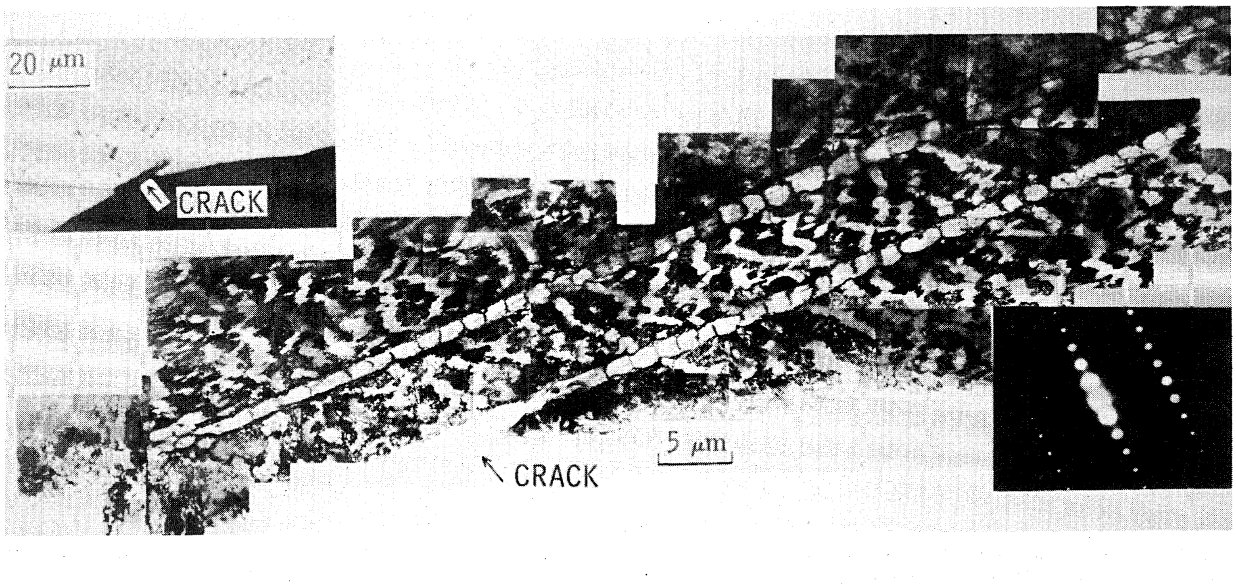

35 Transmission electron micrograph of stage I small cracks propagating within persistent slip bands, showing ladder-like dislocation substructures in fatigued, polycrystalline, high purity copper. Insets show corresponding optical micrograph of cracks and electron diffraction pattern[148]

assume even greater significance in the future since, with improvements in the science and practice of non-destructive testing, the projected lifetime of a fatigue flaw in the short crack regime will become an increasingly larger proportion of the total life.

ACKNOWLEDGMENTS

The work was performed under Grant No. AFOSR-82-0181 from the US Air Force Office of Scientific Research to the University of California at Berkeley. The authors wish to thank Dr A. H. Rosenstein of AFOSR for his support and encouragement, Drs W. L. Morris and J. Lankford for kindly supplying original micrographs, and M. Penton for her help in preparing the manuscript. This review is an expanded version of a paper presented at the 55th Specialists Meeting of the AGARD Structural Materials Panel in Toronto, Canada, in September 1982.

REFERENCES

1. L. F. Coffin: in 'Fatigue and microstructure', (ed. M. Meshii), 1; 1979, Metals Park, Ohio, American Society for Metals.
2. M. R. Mitchell: in 'Fatigue and microstructure', (ed. M. Meshii), 385; 1979, Metals Park, Ohio, American Society for Metals.
3. J. E. Campbell, W. E. Berry, and C. E. Feddersen: 'Damage tolerant design handbook'; 1972, Columbus, Ohio, Metals and Ceramics Information Center, Battelle Columbus Laboratories.
4. S. T. Rolfe and J. M. Barsom: 'Fracture and fatigue control in structures: applications of fracture mechanics'; 1977, Englewood Cliffs, NJ, Prentice Hall.
5. H. H. Johnson and P. C. Paris: *Eng. Fract. Mech.*, 1968, **1**, 3.
6. R. O. Ritchie: *Int. Met. Rev.*, 1979, **24**, 205.
7. M. E. Fine and R. O. Ritchie: in 'Fatigue and microstructure', (ed. M. Meshii), 245; 1979, Metals Park, Ohio, American Society for Metals.
8. S. J. Hudak: *J. Eng. Mater. Technol.* (*Trans. ASME H*), 1981, **103**, 26.
9. M. H. El Haddad, T. H. Topper, and B. Mukherjee: *J. Test. Eval.*, 1981, **9**, 65.
10. J. Schijve: in 'Fatigue thresholds', (ed. J. Bäcklund *et al.*), Vol. 2, 881; 1982, Warley, West Midlands, Engineering Materials Advisory Services Ltd.
11. R. P. Gangloff: in 'Advances in crack length measurement', (ed. C. J. Beevers), 175; 1983, Warley, West Midlands, Engineering Materials Advisory Services Ltd.
12. R. O. Ritchie and S. Suresh: in 'Behaviour of short cracks in airframe components', AGARD Conf. Proc. No. 328, 1-1; 1983, Neuilly sur Seine, Advisory Group for Aerospace Research and Development.
13. M. L. Williams: *J. Appl. Mech.* (*Trans. ASME E*), 1957, **24**, 109.
14. G. R. Irwin: *J. Appl. Mech.* (*Trans. ASME*), 1957, **24**.
15. P. C. Paris and F. Erdogan: *J. Basic Eng.* (*Trans. ASME D*), 1963, **85**, 528.
16. J. R. Rice: in 'Fracture: an advanced treatise', (ed. H. Liebowitz), Vol. 2, 191; 1968, New York, Academic Press.
17. J. R. Rice: in 'Fatigue crack propagation', STP 415, 247; 1967, Philadelphia, Pa, American Society for Testing and Materials.
18. H. Tada, P. C. Paris, and G. R. Irwin: 'The stress analysis of cracks handbook'; 1973, Hellertown, Pa, Del Research Corp.
19. G. C. Sih: 'Handbook of stress intensity factors'; 1973, Bethlehem, Pa, Lehigh University.
20. D. P. Rooke and D. J. Cartwright: 'Compendium of stress intensity factors'; 1975, London, HMSO.
21. N. E. Dowling: *Fatigue Eng. Mater. Struct.*, 1979, **2**, 129.
22. R. O. Ritchie: *J. Eng. Mater. Technol.* (*Trans. ASME, H*), 1983, **105**, 1.
23. J. W. Hutchinson: *J. Mech. Phys. Solids*, 1968, **16**, 13.
24. J. R. Rice and G. R. Rosengren: *J. Mech. Phys. Solids*, 1968, **16**, 1.
25. J. R. Rice: *J. Appl. Mech.* (*Trans. ASME*), 1968, **35**, 379.
26. N. E. Dowling: in 'Cracks and fracture', STP 601, 19; 1976, Philadelphia, Pa, American Society for Testing and Materials.
27. N. E. Dowling and J. A. Begley: in 'Mechanics of crack growth', STP 590, 82; 1976, Philadelphia, Pa, American Society for Testing and Materials.
28. J. W. Hutchinson and P. C. Paris: in 'Elastic–plastic fracture', STP 668, 37; 1979, Philadelphia, Pa, American Society for Testing and Materials.
29. D. M. Parks: unpublished work, Yale University, 1978.
30. C. F. Shih: *J. Mech. Phys. Solids*, 1981, **29**, 305.
31. D. Broek and B. N. Leis: in 'Materials, experimentation and design in fatigue', (ed. F. Sherratt and J. B. Sturgeon), 129; 1981, Guildford, Westbury House.
32. R. O. Ritchie and S. Suresh: *Mater. Sci. Eng.*, 1983, **57**, L27.
33. C. J. Beevers (ed.): 'The measurement of crack length and shape during fracture and fatigue'; 1980, Warley, West Midlands, Engineering Materials Advisory Services Ltd.
34. C. J. Beevers (ed.): 'Advances in crack length measurement'; 1983, Warley, West Midlands, Engineering Materials Advisory Services Ltd.
35. ASTM Standard E647-83 on 'Test method for constant-load-amplitude fatigue crack growth rates above 10^{-8} m/cycle', Annual Book of ASTM Standards, Section 3, 710; 1983, Philadelphia, Pa, American Society for Testing and Materials.
36. W. L. Morris, M. R. James, and O. Buck: in 'Nondestructive evaluation – microstructural characterization and reliability strategies', (ed. O. Buck and S. M. Wolf), 387; 1981, Warrendale, Pa, Metallurgical Society of AIME.
37. J. M. Barsom and R. C. McNicol: in 'Fracture toughness and slow stable cracking', STP

559, 183; 1974, Philadelphia, Pa, American Society for Testing and Materials.
38. Y.H.Kim, T.Mura, and M.E.Fine: *Metall. Trans.*, 1978, **9A**, 1679.
39. C.Y.Kung and M.E.Fine: *Metall. Trans.*, 1979, **10A**, 603.
40. W.L.Morris: *Metall. Trans.*, 1977, **8A**, 589.
41. W.L.Morris and O.Buck: *Metall. Trans.*, 1977, **8A**, 597.
42. W.L.Morris: *Metall. Trans.*, 1978, **9A**, 1345.
43. R.Chang, W.L.Morris, and O.Buck: *Scr. Metall.*, 1979, **13**, 191.
44. W.L.Morris: *Metall. Trans.*, 1979, **10A**, 5.
45. W.L.Morris: personal communication, Rockwell International Science Center, Thousand Oaks, Cal., 1983.
46. W.L.Morris: *Metall. Trans.*, 1980, **11A**, 1117.
47. W.L.Morris, M.R.James, and O.Buck: *Metall. Trans.*, 1981, **12A**, 57.
48. M.R.James and W.L.Morris: *Metall. Trans.*, 1983, **14A**, 153.
49. W.L.Morris, M.R.James, and O.Buck: *Eng. Fract. Mech.*, 1983, **18**, 871.
50. G.P.Sheldon, T.S.Cook, T.W.Jones, and J. Lankford: *Fatigue Eng. Mater. Struct.*, 1981, **3**, 219.
51. N.E.Dowling: in 'Cyclic stress—strain and plastic deformation aspects of fatigue crack growth', STP 637, 97; 1977, Philadelphia, Pa, American Society for Testing and Materials.
52. N.E.Dowling: in Proc. ASME 4th Natl Congr. on 'Pressure vessel and piping technology', Portland, Oreg., June 1983, American Society for Mechanical Engineers.
53. R.P.Gangloff: in 'Fatigue crack growth measurement and data analysis', (ed. Hudak and Bucci), STP 738, 120; 1981, Philadelphia, Pa, American Society for Testing and Materials.
54. R.P.Gangloff: *Res Mech. Lett.*, 1981, **1**, 299.
55. M.T.Resch, D.V.Nelson, J.C.Shyne, and G.S.Kino: in Ref. 34, p. 473.
56. W.Baxter: *Int. J. Fatigue*, 1983, **5**, 37.
57. R.P.Gangloff: in 'Embrittlement by the localized crack environment', (ed. R.P. Gangloff); 1984, Warrendale, Pa, Metallurgical Society of AIME, in the press.
58. B.Wiltshire and J.F.Knott: *Int. J. Fract.*, 1980, **16**, R21.
59. S.Usami and S.Shida: *Fatigue Eng. Mater. Struct.*, 1979, **1**, 471.
60. J.F.McCarver and R.O.Ritchie: *Mater. Sci. Eng.*, 1982, **55**, 63.
61. K.Tanaka and Y.Nakai: *Fatigue Eng. Mater. Struct.*, 1983, **6**, 315.
62. J.Byrne and T.V.Duggan: in 'Fatigue thresholds', (ed. J.Bäcklund *et al.*), Vol. 2, 753; 1982, Warley, West Midlands, Engineering Materials Advisory Services Ltd.
63. S.Suresh: *Eng. Fract. Mech.*, 1984, **20**, in the press.
64. K.Tanaka and Y.Nakai: *J. Eng. Mater. Technol.* (*Trans. ASME H*), 1984, **106**, 192.
65. J.Lankford and D.L.Davidson: *Acta Metall.*, 1983, **31**, 1273.
66. J.Lankford and D.L.Davidson: *Fatigue Eng. Mater. Struct.*, 1983, **6**, 241.
67. F.Guiu, R.Dulniak, and B.C.Edwards: *Fatigue Eng. Mater. Struct.*, 1982, **5**, 311.
68. S.Pearson: *Eng. Fract. Mech.*, 1975, **7**, 235.
69. O.N.Romaniv, V.N.Siminkovich, and A.N. Tkach: in 'Fatigue thresholds', (ed. J.Bäcklund *et al.*), Vol. 2, 799; 1982, Warley, West Midlands, Engineering Materials Advisory Services Ltd.
70. K.Tanaka, M.Hojo, and Y.Nakai: in 'Fatigue mechanisms: advances in quantitative measurement of fatigue damage', (ed. Lankford *et al.*), STP 811, 207; 1983, Philadelphia, Pa, American Society for Testing and Materials.
71. J.Lankford: *Fatigue Eng. Mater. Struct.*, 1982, **5**, 233.
72. J.Lankford: *Fatigue Eng. Mater. Struct.*, 1983, **6**, 15.
73. D.Taylor and J.F.Knott: *Fatigue Eng. Mater. Struct.*, 1981, **4**, 147.
74. C.W.Brown and M.A.Hicks: *Fatigue Eng. Mater. Struct.*, 1983, **6**, 67.
75. Y.Nakai and K.Tanaka: in 'Proc. 23rd Japan congress on materials research', 1980, 106.
76. K.Tanaka, Y.Nakai, and M.Yamashita: *Int. J. Fract.*, 1981, **17**, 519.
77. R.O.Ritchie: *J. Eng. Mater. Technol.* (*Trans. ASME H*), 1977, **99**, 195.
78. J.Lankford: *Eng. Fract. Mech.*, 1977, **9**, 617.
79. S.Taira, K.Tanaka, and M.Hoshina: in 'Fatigue mechanisms', STP 675, 135; 1979, Philadelphia, Pa, American Society for Testing and Materials.
80. S.Taira, K.Tanaka, and Y.Nakai: *Mech. Res. Commun.*, 1978, **5**, 375.
81. S.Suresh: *Metall. Trans.*, 1983, **14A**, 2375.
82. H.Kitagawa and S.Takahashi: in 'Proc. 2nd int. conf. on mechanical behavior of materials', 627; 1976, Metals Park, Ohio, American Society for Metals.
83. D.Taylor: *Fatigue Eng. Mater. Struct.*, 1982, **5**, 305.
84. M.H.El Haddad, K.N.Smith, and T.H.Topper: *J. Eng. Mater. Technol.* (*Trans. ASME H*), 1979, **101**, 42.
85. R.C.Boettner, C.Laird, and A.J.McEvily: *Trans. AIME*, 1965, **233**, 379.
86. H.D.Solomon: *J. Mater.*, 1972, **7**, 299.
87. J.R.Haigh and R.P.Skelton: *Mater. Sci. Eng.*, 1978, **36**, 133.
88. M.S.Starkey and R.P.Skelton: *Fatigue Eng. Mater. Struct.*, 1982, **5**, 329.
89. M.H.El Haddad, T.H.Topper, and K.N.Smith: *Eng. Fract. Mech.*, 1979, **11**, 573.
90. M.H.El Haddad, T.H.Topper, and K.N.Smith: *J. Test. Eval.*, 1980, **8**, 301.
91. M.H.El Haddad, N.E.Dowling, T.H.Topper, and K.N.Smith: *Int. J. Fract.*, 1980, **16**, 15.
92. H.Ohuchida, A.Nishioka, and S.Usami: in 'Proc. 3rd int. conf. on fracture', April 1973, Munich, Verein Deutscher Eisenhüttenlente, Vol. 5, V-443/A.
93. H.Ohuchida, S.Usami, and A.Nishioka: *Bull. Jpn Soc. Mech. Eng.*, 1975, **18**, 1185.
94. S.Usami: in 'Fatigue thresholds', (ed. J. Bäcklund *et al.*), Vol. 1, 205; 1982, Warley, West Midlands, Engineering Materials Advisory Services Ltd.
95. H.Neuber: *J. Appl. Mech.* (*Trans. ASME H*), 1961, **28**, 544.
96. R.E.Peterson: 'Stress concentration factors'; 1974, New York, Wiley—Interscience.
97. R.E.Peterson: in 'Metal fatigue', (ed. G.Sines

and J.L.Waisman), 293; 1959, New York, McGraw-Hill.

98. T.H.Topper, R.M.Wetzel, and J.Morrow: *J.Met.*, 1969, **4**, 200.

99. N.E.Dowling, W.R.Brose, and W.K.Wilson: 'Fatigue under complex loading — analysis and experiments', 55; 1977, Warrendale, Pa, Society of Automotive Engineers.

100. R.A.Smith and K.J.Miller: *Int.J.Mech.Sci.*, 1977, **19**, 11.

101. N.E.Dowling: in 'Fracture mechanics', STP 677, 247; 1979, Philadelphia, Pa, American Society for Testing and Materials.

102. H.Kitagawa: in 'Fatigue thresholds', (ed. J. Bäcklund *et al.*), Vol. 2, 1051; 1982, Warley, West Midlands, Engineering Materials Advisory Services Ltd.

103. P.Lukáš and M.Klesnil: *Mater.Sci.Eng.*, 1978, **34**, 61.

104. M.H.El Haddad, K.N.Smith, and T.H.Topper: in 'Fracture mechanics', STP 677, 274; 1979, Philadelphia, Pa, American Society for Testing and Materials.

105. T.H.Topper and M.H.El Haddad: in 'Fatigue thresholds', (ed. J.Bäcklund *et al.*), Vol. 2, 777; 1982, Warley, West Midlands, Engineering Materials Advisory Services Ltd.

106. C.E.Phillips: in 'Proc. colloq on fatigue', 1955, Stockholm, IUTUM, 210; 1956, Berlin, Springer.

107. N.E.Frost: *J.Mech.Eng.Sci.*, 1960, **2**, 109.

108. N.E.Frost and D.S.Dugdale: *J.Mech.Phys. Solids*, 1957, **5**, 182.

109. M.M.Hammouda and K.J.Miller: in 'Elastic—plastic fracture', STP 668, 703; 1979, Philadelphia, Pa, American Society for Testing and Materials.

110. B.N.Leis and T.P.Forte: in 'Fracture mechanics', STP 743, (ed. R.Roberts), 100; 1981, Philadelphia, Pa, American Society for Testing and Materials.

111. N.E.Frost, K.J.Marsh, and L.P.Pook: 'Metal fatigue'; 1974, Oxford, Clarendon Press.

112. W.Elber: in 'Damage tolerance in aircraft structures', STP 486, 230; 1971, Philadelphia, Pa, American Society for Testing and Materials.

113. K.Endo, K.Komai, and Y.Matsuda: *Mem. Fac.Eng., Kyoto Univ.*, 1969, **31**, 25.

114. R.O.Ritchie, S.Suresh, and C.M.Moss: *J.Eng.Mater. Technol.* (*Trans.ASME H*), 1980, **102**, 293.

115. A.T.Stewart: *Eng.Fract.Mech.*, 1980, **13**, 463.

116. S.Suresh, G.F.Zamiski, and R.O.Ritchie: *Metall.Trans.*, 1981, **12A**, 1435.

117. N.Walker and C.J.Beevers: *Fatigue Eng. Mater.Struct.*, 1979, **1**, 135.

118. K.Minakawa and A.J.McEvily: *Scr.Metall.*, 1981, **15**, 633.

119. R.O.Ritchie and S.Suresh: *Metall.Trans.*, 1982, **13A**, 937.

120. S.Suresh and R.O.Ritchie: *Metall.Trans.*, 1982, **13A**, 1627.

121. S.Suresh, D.M.Parks, and R.O.Ritchie: in 'Fatigue thresholds', (ed. J.Bäcklund *et al.*), Vol. 1, 391; 1982, Warley, West Midlands, Engineering Materials Advisory Services Ltd.

122. S.Suresh and R.O.Ritchie: *Scr.Metall.*, 1983, **17**, 575.

123. R.A.Schmidt and P.C.Paris: in 'Progress in flaw growth and fracture toughness testing', STP 536, 79; 1973, Philadelphia, Pa, American Society for Testing and Materials.

124. R.O.Ritchie, S.Suresh, and P.K.Liaw: in 'Ultrasonic fatigue', (ed. J.M.Wells *et al.*), 433; 1982, Warrendale, Pa, Metallurgical Society of AIME.

125. S.Suresh and R.O.Ritchie: in 'Concepts of fatigue crack growth thresholds', (ed. D.L. Davidson and S.Suresh), 227; 1984, Warrendale, Pa, Metallurgical Society of AIME.

126. S.Suresh: *Scr.Metall.*, 1982, **16**, 995.

127. S.Suresh: *Eng.Fract.Mech.*, 1983, **18**, 577.

128. S.Suresh and A.K.Vasudévan: in 'Concepts of fatigue crack growth thresholds', (ed. D.L. Davidson and S.Suresh); 361; 1984, Warrendale, Pa, Metallurgical Society of AIME.

129. R.J.Cooke, P.E.Irving, G.S.Booth, and C.J. Beevers: *Eng.Fract.Mech.*, 1975, **7**, 69.

130. B.F.Jones: *J.Mater.Sci.*, 1982, **17**, 499.

131. K.J.Miller: *Fatigue Eng.Mater.Struct.*, 1982, **5**, 223.

132. W.T.Chiang and K.J.Miller: *Fatigue Eng. Mater.Struct.*, 1982, **5**, 249.

133. A.Talug and K.Reifsnider: in 'Cyclic stress—strain and plastic deformation aspects of fatigue crack growth', STP 637, 81; 1977, Philadelphia, Pa, American Society for Testing and Materials.

134. R.J.Allen and J.C.Sinclair: *Fatigue Eng. Mater Struct.*, 1982, **5**, 343.

135. J.C.Newman, Jr: in 'Behaviour of short cracks in airframe components', AGARD Conf. Proc. No. 328, 6-1; 1983, Neuilly sur Seine, Advisory Group for Aerospace Research and Development.

136. T.Kunio and K.Yamada: in 'Fatigue mechanism', STP 675, 342; 1979, Philadelphia, Pa, American Society for Testing and Materials.

137. B.A.Bilby, C.E.Cardew, and I.C.Howard: in 'Fracture 1977', (ed. D.M.R.Taplin), Vol. 3, 197; New York, Pergamon.

138. B.Cotterell and J.R.Rice: *Int.J.Fract.*, 1980, **16**, 155.

139. P.J.E.Forsyth: in 'Crack propagation', 76; 1962, Cranfield, Bedfordshire, Cranfield Press.

140. R.M.McMeeking and A.G.Evans: *J.Am. Ceram.Soc.*, 1982, **65**, 242.

141. J.M.Potter and B.G.W.Yee: in 'Behaviour of short cracks in airframe components', AGARD Conf. Proc. No. 328, 4-1; 1983, Neuilly sur Seine, Advisory Group for Aerospace Research and Development.

142. K.A.Esaklul, A.G.Wright, and W.W. Gerberich: *Scr.Metall.*, 1983, **17**, 1073.

143. C.Laird: 'Fatigue and microstructure', (ed. M.Meshii), 149; 1979, Metals Park, Ohio, American Society for Metals.

144. H.Mughrabi: in 'Strength of metals and alloys', (ed. P.Haasen et al.), Vol. 3, 1615; 1980, New York, Pergamon.

145. G.Lütjering, H.Döker, and D.Munz: in 'The microstructure and design of alloys', Vol. 1, 427; 1973, London, The Institute of